NASA/CR–2011-217077

Measured Sonic Boom Signatures Above and Below the XB-70 Airplane Flying at Mach 1.5 and 37,000 Feet

Domenic J. Maglieri and Herbert R. Henderson
Eagle Aeronautics, Inc., Hampton, Virginia

Ana F. Tinetti
NCI Information Systems, Inc., Hampton, Virginia

April 2011

NASA STI Program . . . in Profile

Since its founding, NASA has been dedicated to the advancement of aeronautics and space science. The NASA scientific and technical information (STI) program plays a key part in helping NASA maintain this important role.

The NASA STI program operates under the auspices of the Agency Chief Information Officer. It collects, organizes, provides for archiving, and disseminates NASA's STI. The NASA STI program provides access to the NASA Aeronautics and Space Database and its public interface, the NASA Technical Report Server, thus providing one of the largest collections of aeronautical and space science STI in the world. Results are published in both non-NASA channels and by NASA in the NASA STI Report Series, which includes the following report types:

- TECHNICAL PUBLICATION. Reports of completed research or a major significant phase of research that present the results of NASA programs and include extensive data or theoretical analysis. Includes compilations of significant scientific and technical data and information deemed to be of continuing reference value. NASA counterpart of peer-reviewed formal professional papers, but having less stringent limitations on manuscript length and extent of graphic presentations.

- TECHNICAL MEMORANDUM. Scientific and technical findings that are preliminary or of specialized interest, e.g., quick release reports, working papers, and bibliographies that contain minimal annotation. Does not contain extensive analysis.

- CONTRACTOR REPORT. Scientific and technical findings by NASA-sponsored contractors and grantees.

- CONFERENCE PUBLICATION. Collected papers from scientific and technical conferences, symposia, seminars, or other meetings sponsored or co-sponsored by NASA.

- SPECIAL PUBLICATION. Scientific, technical, or historical information from NASA programs, projects, and missions, often concerned with subjects having substantial public interest.

- TECHNICAL TRANSLATION. English-language translations of foreign scientific and technical material pertinent to NASA's mission.

Specialized services also include creating custom thesauri, building customized databases, and organizing and publishing research results.

For more information about the NASA STI program, see the following:

- Access the NASA STI program home page at *http://www.sti.nasa.gov*

- E-mail your question via the Internet to help@sti.nasa.gov

- Fax your question to the NASA STI Help Desk at 443-757-5803

- Phone the NASA STI Help Desk at 443-757-5802

- Write to:
  NASA STI Help Desk
  NASA Center for AeroSpace Information
  7115 Standard Drive
  Hanover, MD 21076-1320

NASA/CR–2011-217077

Measured Sonic Boom Signatures Above and Below the XB-70 Airplane Flying at Mach 1.5 and 37,000 Feet

Domenic J. Maglieri and Herbert R. Henderson
Eagle Aeronautics, Inc., Hampton, Virginia

Ana F. Tinetti
NCI Information Systems, Inc., Hampton, Virginia

National Aeronautics and
Space Administration

Langley Research Center
Hampton, Virginia 23681-2199

Prepared for Langley Research Center
under Contract NNL07AE38T

April 2011

Available from:

NASA Center for AeroSpace Information
7115 Standard Drive
Hanover, MD 21076-1320
443-757-5802

Measured Sonic Boom Signatures Above and Below the XB-70 Airplane Flying at Mach Number 1.5 and 37,000 Feet

By Domenic J. Maglieri and
Herbert R. Henderson and Ana F. Tinetti

ABSTRACT

During the 1966-67 Edwards Air Force Base (EAFB) National Sonic Boom Evaluation Program, a series of in-flight flow-field measurements were made above and below the USAF XB-70 using an instrumented NASA F-104 aircraft with a specially designed nose probe. These were accomplished on three XB-70 flights conducted at a Mach number of about 1.5 at an altitude of about 37,000 feet and at a gross weight of about 350,000 pounds. A total of six supersonic passes were made with the F-104 probe aircraft through the XB-70 shock flow-field; one above the XB-70 on the first flight, two below the XB-70 on the second flight, and three below the XB-70 on the third flight. Separation distances ranged from about 3000 feet above and 7000 feet to the side of the generating aircraft and about 2000 feet and 5000 feet below the generating aircraft. Complex near-field "sawtooth-type" signatures were observed in all cases. In fact, at ground level, the XB-70 shock waves had not coalesced into the two-shock classical sonic boom N-wave signature, but contained three shocks.

The purpose of these in-flight measurements was to gather an additional database on a very large and heavy aircraft to be used in providing a check on and improvement to the generalized theory for predicting sonic boom signatures. Although the tests were successfully completed, the results were never formally documented appearing, only briefly, in a few reports to reflect the nature of the flight tests.

The present report documents the results of the XB-70/F-104 probe flight tests and is based upon file copies of most of the original information and database developed in the 1966-67 time period. Included in this report is a description of the generating and probe airplanes, details of the in-flight and ground pressure measuring instrumentation, the flight test procedure and the aircraft in-flight and ground pressure measuring instrumentation, the flight test procedure and aircraft positioning, surface and upper air weather observations and the six measured in-flight pressure time histories from the three XB-70 flights along with the corresponding ground measured signatures.

THIS PAGE INTENTIONALLY LEFT BLANK

TABLE OF CONTENTS

INTRODUCTION - 7
SYMBOLS - 8
APPARATUS AND METHODS - 9
Generating and Probe Airplanes - 9
Pressure Measuring Instrumentation - 10
Flight Test Procedures - 10
Aircraft Positioning - 11
Weather Observations - 12
RESULTS - 12
Inflight Measurements - 12
Wave Shapes - 12
Peak Positive Overpressures - 14
Signature lengths - 15
Ground Measurements - 15
Microphone Set-Up and Characteristics - 15
Wave Shapes - 16
Signature Characteristics - 16
Correlation with Airplane Geometry - 16
SUMMARY REMARKS - 17
APPENDIX A
DESCRIPTION AND CALIBRATION OF PRESSURE INSTRUMENTATION - 18
APPENDIX B
DESIGN AND AERODYNAMICS CALIBRATION OF PRESSURE PROBE - 20
Basic Considerations - 20
Present Applications - 20
WIND TUNNEL TESTS - 21
Introduction - 21
Symbols - 21
Apparatus and Tests - 22
Test facility and conditions - 22
Test apparatus and procedures - 22
Measurements - 23
Data and Precision - 23
Probe Calibration - 23
Pressure measurements in vicinity of oblique shock wave - 23
Results and Discussion - 23
Probe calibration at angle of attack - 23
Probe capability for sensing pressure changes across an oblique shock wave - 24
Probe reflection factors for correcting in-flight measurements - 25
General comments - 25

REFERENCES - 26

LIST OF TABLES

Table 1 Geometric characteristics of XB-70 airplane 29

Table II Summary of XB-70 and F-104 in-flight probe test conditions 34

Table III XB-70 flight conditions overhead of ground cruciform microphone array 35

Table IV Upper air atmospheric data 36

Table V Surface weather observations at EAFB runway 22/04 39

Table VI Summary of XB-70 maximum positive overpressures, signature lengths and periods for in-flight probe tests 40

Table VII XB-70 sonic boom signature characteristics measured at ground level with the six microphone cruciform array 41

LIST OF FIGURES

Figure 1 Photograph of XB-70 delta wing supersonic aircraft used as the sonic boom generator in the present studies 42

Figure 2 Three view drawing of XB-70 airplane 43

Figure 3 Photograph of XB-70 showing windshield-nose ramp positions 44

Figure 4 Area distribution of XB-70-1 vehicle used as shock-wave generation airplane 45

Figure 5 F-104 airplane with nose-boom probe installation for measuring the shock flow-field in the vicinity of the disturbance generating XB-70-1 airplane 46

Figure 6 Photographs of the in-flight recording instrumentation mounted in the F-104 access bay 47

Figure 7 Principal details and dimensions of full-scale probe used for in-flight measurements and for wind tunnel tests at a Mach number of about 2.01 48

Figure 8 Adaptor required to mate specially instrumented noise-boom pressure probe used originally on an F-106 to the NASA F-104 used in present tests 49

Figure 9 Schematic of XB-70 and F104 nominal ground tracks showing area in which probe missions were flown and ground measurements were acquired 50

Figure 10 Sketches illustrating general position of probe aircraft and generating aircraft 51

Figure 11 Copy of November 23, 1966 film trace showing in-flight time histories of differential pressures measured in flow-field above XB-70 aircraft 52

Figure 12 Copy of December 12, 1966 film trace showing in-flight time histories of differential pressures measured in flow-field below the XB-70 aircraft 53

Figure 13 Copy of December 16, 1966 film trace showing in-flight time histories of differential pressures measured in flow-field below XB-70 aircraft 54

Figure 14 XB-70 flow-field shock-wave signature overpressures 55

Figure 15 Comparison of measured and calculated distance between bow-wave and tail-wave of generating airplane 57

Figure 16 XB-70 measured sonic boom signatures at ground level following in-flight probe tests 58

Figure 17 Diagrams of waveforms and signature characteristics which represent the various categories of measured sonic booms 59

Figure 18 Planform and side views of bomber airplane with time history of pressure signature as measured above and below airplane. Signature length has been adjusted to made distance between nose and tail shocks approximately the same as the airplane lengths .60

Figure 19 Response characteristics of pressure instrumentation use for in-flight measurements 61

Figure 20 Steady-state calibration of flight probe at angles-of-attack from -2.5^{o} to 9.5^{o}, as obtained from tests in the Langley 4-foot supersonic pressure tunnel (pressure orifices at bottom of probe). $M_\infty \approx p_\infty \approx 185$ lbs/ft^2 62

Figure 21 Wind-tunnel apparatus and test arrangement for generating and determining the strength of an axisymmetrical disturbance used in obtaining experimental evidence concerning the reflection characteristics of the flight probe 63

Figure 22 Flight-probe capability for sensing static-pressure changes across an axisymmetrical disturbance (bow wave generated by body of revolution), as evidenced by comparison of probe-indicated, survey-indicated, and estimated pressure changes across bow-wave, $M_\infty \approx 2.01$ 65

INTRODUCTION

Verification of existing and newly-developed sonic boom prediction codes required an experimental database consisting of sonic boom pressure signatures measured at ground level and also by probing the supersonic flow-field above, below, and to the side of the generating airplane. A majority of the ground measurements are acquired at airplane altitude, Mach conditions such that all of the shocks within the supersonic flow field have coalesced into the classical N-wave sonic boom signature (ref. 1-3). In addition, the atmospheric through which these shock waves propagate, especially the lower layers, can strongly alter this N-wave shape such that peaked or rounded waveforms are observed with the resulting large variations in sonic boom overpressures as compared to “clean” N-waves observed under “quiescent” atmospheric conditions (refs. 1-4). Complex near-field sonic boom signatures have been measured at ground level for flights of aircraft at very low altitudes where multiple shocks are experienced and the signature takes on a “sawtooth” appearance (refs. 5 and 6).

In-flight flow-field measurements, on the other hand, are not significantly influenced by the atmosphere through which they propagate, especially if the separation distances between the generating and probing aircraft are small. In addition, these near-field signatures are more complex in that they indicate the shock patterns well before they have coalesced into the single bow and tail shock typical of the classical far-field N-wave. Thus, they provide for a critical test of the predictive codes.

The in-flight supersonic flow-field database has been gathered over four decades. In 1956 the United States Air Force (USAF) conducted flight tests of an F-100 probing below and to the side of an F-100 generating airplane at distances of from about 2 to 41 body lengths (ref. 7). In 1960 this was followed by a series of in-flight measurements by NASA using an F-100 to probe very close to the side of an F-100, F-104 and B-58 airplane at separation distances of from 1 to 8 body lengths (ref. 8). In 1963 the USAF and NASA extended this in-flight database by probing the flow-field above and below the B-58 with an F-106 which incorporated a specially designed and instrumented nose probe at distances of from about 14 to 95 body lengths (ref. 9). During the 1966-1967 Edwards Air Force Base (EAFB) National Sonic Boom Evaluation Program, the opportunity was taken to acquire near-field signatures above and below the very large and heavy USAF XB-70 airplane using a NASA F-104 (ref. 10) airplane equipped with the same specially instrumented nose probe used on the F-106/B-58 tests of 1963. Separation distances of from about 10 to 42 body lengths were experienced. During the 1995 time period, NASA conducted an extensive series of in-flight probe measurements using the SR-71 as the generating airplane and the F-16XL as the probing airplane. A significant number of flow-field penetrations were made at distances of from about 5 to 76 body lengths below the SR-71 with the F-16XL and the distances to about 200-300 body lengths below the SR-71 using an instrumented YO3A subsonic airplane and at ground level (ref. 11). The SR-71 flight tests were part of the NASA High Speed Research (HSR) Program aimed at establishing the technology base for any future High Speed Civil Transport (HSCT). The most recent in-flight probe tests were conducted using a USN F-5E aircraft which was reshaped to produce a flat-top sonic boom signature at the ground. These measurements were part of the 2003 DARPA Shaped Sonic Boom Demonstrator Program (SSBD) and the 2004 NASA Shaped Sonic Boom Experiments Program (SSBE).[1]

[1]Pawlowski, J. W.; Graham, D. H.; Boccadoro, C.H.; Coen, P.G. and Maglieri, D.J.: “Origins and Overview of the Shaped Sonic Boom Demonstration Program,” AIAA 2005-0005, January 2005.

With the exception of the 1960 NASA probe tests (ref. 8), the NASA SR-71 in-flight flow-field data (ref. 11) and the SSBD and SSBE measurements, little use has been made of the 1963 and 1966 probe measurements of the B-58 and XB-70 flow-field signature data in terms of theory validation. This is due, in part, to the lack of sufficient details of the B-58 and XB-70 geometric and aerodynamic description which has recently been generated (ref. 12) and the availability of the details of the XB-70 measurements (the B-58 tests are reported in full detail in ref. 9). Although the XB-70/F104 in-flight probe measurement effort was successfully completed, the results were never formally documented, appearing only briefly in a few reports in preliminary form (refs. 10, 13-15) to reflect the general nature of the flight test results.

The present report documents the results of the XB-70 and F-104 flight tests and is based upon file copies of most of the original information and database developed in the 1966-1967 time period. Included in this report is a description of the generating and probe airplanes, details of the in-flight and ground pressure measurement instrumentation, the flight tests procedures and aircraft positioning, surface and upper air weather observations, and the six measured in-flight pressure time histories from the three XB-70 flights along with the corresponding ground measured signatures.

Since the nose probe pressure instrumentation used on the NASA F-104 aircraft is the same as that used on the USAF F-106 for the NASA-USAF B-58 probe tests (ref. 9), Appendices A and B, taken from reference 9, are also included in this report. Appendix A, by John F. Bryant, Jr., provides a description and static calibration of the pressure instrumentation, and Appendix B, by Virgil S. Ritchie, gives a detailed description of the unique instrumentation probe used to obtain the pressure measurements along with the corresponding static and wind tunnel calibrations.

Since the flight experiments, objectives and flight-test techniques of both the 1966 XB-70/F-104 and the 1963 B-58/F-106 probe tests were similar, the report format utilized in the B-58/F-106 report (ref. 9) will be used for the present report. In addition, calculations of the XB-70 sonic boom overpressures, period, and signature lengths will be made using the predictive scheme available at the time of the flight tests.

SYMBOLS

A	area of XB-70-1 airplane section obtained by oblique cut for a nominal Mach number of 1.5, ft.^{2}
h	vertical distance from ground to airplane, ft.
l	length of bomber airplane, ft.
M	airplane Mach number
ΔM	differential Mach number between generating and probe airplanes
Δp_{max}	peak positive overpressures, lbs/ft^2

r slant range separation distance between generating airplane and probe airplane, measured perpendicular to generating-airplane flight track (positive when probe airplane is below generating airplane), $\sqrt{(Z)^2 + (Y)^2}$, ft.

S horizontal distance of probe airplane behind generating airplane at penetration, ft.

ΔT time interval between bow and tail shock waves of generating airplane in horizontal plane, msec

V airplane ground velocity, ft/sec

ΔV differential ground velocity between generating and probe airplane, ft/sec.

W gross weight of XB-70 airplane, lbs.

X distance between bow and tail shock waves of generating airplane in horizontal plane (signature length), ft.

x axial distance from nose of airplane, ft.

Y lateral separation distance between generating and probe airplanes, ft.

Z vertical separation distance between generating and probe airplanes (positive when probe airplane is below generating airplane), ft.

τ bow shock rise time to maximum overpressure, msec.

$\tau_{1/2}$ bow shock rise time to one-half maximum overpressure, msec.

θ azimuthal position about generating aircraft (defined in fig. 4).

ϕ experimentally determined shock-wave angle of ground level.

APPARATUS AND METHOD

Generating and Probe Airplanes

The USAF XB-70-1 delta-wing airplane, shown on figure 1, was used as the generating vehicle. A three-view drawing of this airplane is shown in figure 2 and detailed geometric characteristics are provided in Table I that is taken from reference 16. The aircraft has a length of 189 feet (including nose boom), a wing span of 105 feet, and a total wing area of 6297.8 square feet. Aircraft weight at brake release for the three probe flights ranged from about 529,000 pounds to 536,000 pounds. During the actual probe runs, the XB-70 gross weight ranged from about 320,000 pounds to 350,000 pounds; wing tips were full down at 65 degrees and the nose ramp windshield was in the down position (see fig. 3). The bypass was set at 400 square inches and all engines were at 100 percent RPM and exhaust nozzles were in partial afterburner. The aircraft is powered by six YJ9-GE-turbojet engines, each producing 31,000 pounds thrust with full after-

burner. Calculated area distributions, based on a Mach 1.5 oblique cut for a position above and to the side of the XB-70 and also positions below the XB-70, are given in figure 4. These area developments correspond to the probe flight measurements contained in this report and were generated using the vehicle geometric description given in reference 12.

The NASA F-104 airplane, shown in figure 5(a), was used with a specially instrumented nose boom probe for sensing pressure changes during flight through the flow-field of the XB-70-1 airplane. The special nose-boom pressure probe is shown in figure 5(b) and is the same probe that was mounted on the USAF F-106 to survey the flow-field above and below the B-58 airplane in 1963 (see ref. 9). Photographs of the in-flight recording instrumentation mounted in the F-104 are shown in figure 6. Included are a carrier amplifier, NASA recording oscillograph, a temperature control box, and a NASA timer. Both the USAF XB-70 and NASA F-104 were based at Edwards Air Force Base, California, the XB-70 being operated by the personnel of the Air Force Flight Test Center (AFFTC) and the F-104 by the NASA Flight Research Center (FRC), now NASA Dryden Flight Research Center (DFRC).

Pressure Measuring Instrumentation

The specially instrumented nose-boom probe was designed, fabricated and calibrated by NASA Langley Research Center personnel. Details of the pressure probe and wind tunnel tests to determine the pressure-sensing characteristics of the probe are described in Appendices A and B of reference 9 and are reproduced in this report for completeness. The general arrangement of main dimensions of the probe components are illustrated schematically in figure 7. (Symbols in figure 7 are defined in Appendix B.) Two NASA inductive-type miniature pressure gages were contained in the probe at locations near pressure-sensing orifices. The probe was laboratory-checked, once again, before installation on the NASA F-104 airplane to reestablish its sensitivity to a vibration environment. For the present flight tests, the pressure probe was fitted with a conical tip (fig. 7). An adapter, shown in figure 8, was required in mating the rear portion of the instrumented probe to the F-104 such that the angle-of-attack of the probe would be near zero degrees for the expected flight conditions.

Flight Test Procedures

As mentioned previously, the XB-70 probe tests were an attachment to the Phase II part of the 1966-1967 EAFB National Sonic Boom Evaluation Program. The general arrangement of the probe flight test plan is provided in figure 9. Probing flights were conducted in “piggy-back” fashion during the XB-70’s sonic boom run over the main test area near the west-end of Rogers Dry Lake where sonic boom ground pressure measurements, building response measurements, and subjective response studies were being conducted (see ref. 17).

To accommodate both the in-flight probe measurements and the ground test site measurements, the XB-70 established a steady flight condition of about Mach 1.5 and 37,000 feet MSL about 100 nautical miles east of the ground test site (just east of Soda Lake) and maintained these conditions flying a nominal 245 degrees magnetic heading (261 deg.true) that brought it over the main test area. Probe flights were to be conducted above and below the XB-70 during its run-in to the main

test area (see fig. 9). If the probe flights were not completed by the time both aircraft were abeam of four corners, the F-104 probe aircraft would break off so as not to boom the test area.

The probe flight plan required the F-104 to be at 2000 to 5000 feet above or below the XB-70 flight altitude and at a Mach 1.3 over Soda Lake awaiting the inbound XB-70 flying at about Mach 1.5 to overtake it. Once the aircraft slipped back through the XB-70 flow field, the F-104 probe aircraft would accelerate to about Mach 1.7 and hold this speed as it penetrated the XB-70 flow-field from rear to front. After completing the penetration, the F-104 reduces to about Mach 1.3 and slides back through the XB-70 flow-field. This sequencing of three surveys of the XB-70 flow field takes about 3 to 4 minutes and some 60 to 70 nautical miles. The speed and altitude of the XB-70 and F-104 were held as steady as possible during penetration; however, the F-104 did experience small variations in velocity which ranged about $\pm$5ft./sec. A maximum of three and a minimum of one F-104 probe penetrations were possible depending upon aircraft coordination positioning and fuel remaining.

The probe pressure-measurement system on the instrumented airplane was kept inert from the time of takeoff until steady flight conditions were established (see Appendix A for details). Just prior to penetration of the pressure field of the generating airplane, the pilot of the F-104 probe airplane was instructed by radio to activate the pressure measurement system. In addition, The F-104 pilot transmitted a timing signal to the ground tracking station both prior to and subsequent to penetration. This timing signal was superimposed on the tracking data and the data record of the flight recorder.

Aircraft Positioning

Positioning and guidance of both the XB-70 and F-104 aircraft was accomplished using two USAF-FPS-16 precision radars operated by AFFTC personnel located at the EAFB radar facility (SPORT). A radar transponder was located on the bottom of the XB-70 and 102 feet behind the nose. The F-104 transponder was located about 10 feet behind the tip of the probe. Accuracies in range, velocity and acceleration were quoted as 40 feet, 10 ft/sec, and 5 ft/sec^2, respectively.

All six (6) probe runs were conducted with the XB-70 flying at nominal conditions of about Mach 1.5 and 37,000 feet MSL and a gross weight of about 340,000 pounds. Figure 10 provides sketches illustrating the general position of the probe aircraft and generating aircraft for the six probe runs. The XB-70 and F-104 coordinate systems at time of penetration is shown in figure 10(a) where S, Y and Z are the distances that the F-104 is behind, to the side, and above or below the XB-70. The distance, r, is the slant range distance of the F-104 from the XB-70 flight axis (for y = 0, r =z). Figure 19(b) provides a rear view, looking in the flight direction, showing the six F-104 probe runs relative to the XB-70 flow field. Note that although the intent was to position the F-104 directly above and directly below the XB-70, only four of the six penetrations were within less than 1000 feet of the vertical. Run 1 of the flight test date, December 16, 1966, was about 3000 feet to the side and the single penetration of flight test date, November 23, 1966, was about 7000 feet to the side of the XB-70 flight track.

A summary of the XB-70 and F-104 in-flight probe test conditions is given in Table II for each of the three test dates for all six probe penetrations. Included is the time of penetration, the XB-70

Mach, altitude, heading, weight, ground speed, canard and elevon positions, the F-104 Mach and altitude, heading and ground speed. Also shown are the S, Y, and Z and r distances of the F-104 from the XB-70 at time of shock penetrating and the closure rate between the XB-70 and F-104 (ΔM and ΔV). The XB-70 pilots experienced light to moderate turbulence on all three probe test dates, and only during one of the six penetrations (Pass 1 on Dec. 16, 1966) did the XB-70 pilot and co-pilot experience a slight bump from the F-104 shock field.
Table III provides a summary of the XB-70 flight conditions overhead of the ground cruciform microphone array at the main test site for the three probe flight test days. The time at overhead of the ground measurement site is some 2 to 5 minutes after the probe flight penetrations. Comparison of the XB-70 flight parameters of Tables I and III indicate the vehicle was essentially at steady-level conditions for the entire run in from Soda Lake some 100 miles east to the main test site at EAFB. The XB-70 ground velocities given in Table III were obtained from the ground microphone cruciform array.

Weather Observations

Both surface and upper air weather observations were made during the 1966-67 EAFB National Sonic Boom Evaluation Program. Rawinsonde observations from the EAFB weather facility include measured values of pressure, temperature, relative humidity and wind speed and direction from near the surface to altitudes well in excess of the aircraft flight altitudes. The Edwards upper air atmospheric data, as archived by the National Climatic Data Center in Asheville, North Carolina, for the days (Nov. 23, Dec. 12 and Dec. 16, 1966) on which the XB-70 probe measurements were conducted is presented in Table IV. The aircraft headings were such that slight to moderate headwinds were encountered at flight altitude on all three XB-70 probe flights.

A summary of the surface weather conditions observed at the Edwards runway 22/04 on the three test days and at the approximate time the XB-70 was overhead of the main test area cruciform microphone array is presented in Table V. Over the three test day mornings, cloud cover ranged from clear to overcast with no precipitation. Winds were calm and temperatures ranged from 27^{o}F to 47^{o}F.

RESULTS

Both the in-flight probe and ground measurements of the shock wave pressure signatures of the XB-70 are presented. Figures 11-15 and Table VI relate to the measured signatures obtained from the six in-flight probe runs and figures 16-17 and Table VII address the measured signatures at the two ground sites for the three XB-70 flights. A correlation of the in-flight and ground pressure time histories with airplane geometry is shown in figure 18.

In-Flight Measurements

Wave shapes. - A copy of the F-104 probe aircraft film trace showing the in-flight time histories of differential pressures measured on all six penetrations on the three XB-70 flights of November 23, December 12, and December 16, 1966 are presented in figures 11, 12, and 13, respectively. In each case, the top pressure trace was obtained with gage 1, which was connected to the forward

orifices on the measuring boom, whereas the bottom trace was obtained with gage 2, which was connected to the rearward orifices (see fig. 7). The two pressure traces are not directly comparable in amplitude because of differences in the sensitivities of the gages and in the reflection factors for the probe at the orifice locations and, possibly, because of effects of boundary layer and airplane angle-of-attack.

True time on the film records of figures 11-13 is represented by right to left direction, thus when the XB-70 was overtaking the F-104 probe airplane, the XB-70 bow-shock is presented first and its tail shock last. At the top of the film were a series of dots at 0.5 sec time intervals (shown where available). However the 0.5 second time interval is indicated for each run. Because of the fore and aft displacement of the two sets of orifices on the probe (about 10-inches), penetration of the rear gage (gage 2) is indicated a very short time ahead of the indication by the front gage (gage 1) during the XB-70 overtake of the F-104, and the reverse is true when the F-104 overtakes the XB-70. The absence of any noticeable oscillations in these pressure time histories, prior to the entrance and following the exit of the probe airplane from the XB-70 flow-field, indicates the probe tip vibrations, experienced on some of the close-in runs on the B-58/F-106 probe tests of 1963 (ref. 9) was not experienced on these flights. Also indicated in figures 11-13 are the estimated lengths of each signature based upon the film timing marks and the closure rate between the XB-70 and F-104 as determined from the radar data and listed in Table II.

On the first probe flight of November 23, the F-104 was able to complete only one penetration which was at a position 3290 feet above and 7100 feet to the left-side of the XB-70. The pressure time histories are shown in figure 11. Examination of the pressure traces indicate the presence of three main shocks with another weaker shock appearing just prior to the tail shock. Note, too, that the gradual downward shift of the ambient levels on both pressure gages prior to the F-104 sliding back through the XB-70 bow shock and continuing throughout the flow-field traverse, indicating a slight change in F-104 altitude during the probe run.

A signature length X of 529 feet is established based upon a closure rate between the two aircraft of 310 ft/sec (see Table II). It should be noted that this signature length is significantly longer than those observed at ground level for the XB-70 flying at the same operating conditions of Mach 1.5 and 35,000 feet altitude. The signature length of the 529-feet results primarily from the 14 degrees difference in headings between the XB-70 (259 deg.true) and F-104 (273 deg.true) aircraft during the time of penetration (see Table II). Thus, the F-104 aircraft probed the XB-70 flow-field on a "skewed" rather than a "parallel" path 3290 feet above and 7100 feet to the left of the XB-70 flight track resulting in a longer signature. In addition to the heading differences, the slight change in the F-104 altitude from the beginning to end of the probe penetration (as indicated by the downward shift of the ambient level signature traces in figure 11 would also contribute to the observed increased signature length.

On the second probe flight of December 12, 1966, the F-104 was able to complete two penetrations of the XB-70 flow-field. The first pass with the XB-70 overtaking the F-104 occurred at a distance of 4727 feet below and 220 feet to the side, and on the second pass the F-104 overtook the XB-70 penetrating the flow-field at a distance of 4656 feet below and 825 feet to the side. The difference in the XB-70 and the F-104 headings during each of these two penetrations was 2 degrees and zero degrees, respectively. Pressure time histories of these two passes are given in

figure 12. It can be seen that these signatures consist of four primary shocks with an additional two secondary shocks. Signature lengths of 198 feet and 220 feet are noted for the two passes based upon closure rates of 155 ft/sec and 344 ft/sec, respectively (see Table II). The difference in flow-field penetration time for the two passes is apparent from the traces.

On the third probe flight of December 16, 1966, the F-104 was able to complete three penetrations of the XB-70 flow-field. The first pass with the XB-70 overtaking the F-104 occurred at a distance of 1870 feet below and 2900 feet to the side. On the second pass, the F-104 overtook the XB-70 penetrating its flow-field at a distance of 2031 feet below and 980 feet to the side. On the third pass, the F-104 slid back through the XB-70 flow-field at a distance of 1802 feet below and 590 feet to the side. The difference in the XB-70 and F-104 headings during each of these three penetrations was 2 degrees, zero degrees, and zero degrees, respectively. The pressure time histories for the three passes are presented in figure 13. It can be seen that from four to five major shocks are evident with as many as four additional secondary shocks. Signature lengths of 252 feet, 211 feet and 188 feet are noted for these three passes based upon closure rates of 268 ft/sec, 153 ft/sec and 103 ft/sec, respectively (see Table II).

Peak positive overpressures. - Following each of the probe flights, the NASA Flight Research Center (now Dryden Flight Research Center) applied the appropriate calibration curves for each of the two gages on each of the three flight test dates to the pressure time histories of figures 11-13 and established the results presented in figure 14. Each of the six flow-field signatures were reconstructed from figures 11 to 13 so that they all begin with the bow-shock and end with the tail-shock. The location of each of the individual shocks are presented as ratio of the total signature which is 100 percent. Gage 1 (front gage) is represented by the solid line and gage 2 (aft gage) by the dashed line. It should be emphasized that the finite shock rise times associated with the signatures of figure 14 are a result of the reconstruction process and, thus, are not a true indication of the actual shock rise time. The main purpose of figure 14 was to assign an absolute overpressure scale to the film trace signatures of figures 11, 12, and 13.

Examination of the signature traces of figure 14 shows that the overpressures measured by gages 1 and 2 are fairly consistent, with somewhat higher values recorded by gage 1 for locations below the XB-70 and slightly higher values observed by gage 2 for the single pass above the aircraft. Peak positive overpressures ranged from about 1.2 lbs/ft^2 at 42 body lengths above and to the side of the XB-70 (fig. 14a) to as high as 5.0 lbs/ft^2 at 10 body lengths below the aircraft (fig. 14f). In all but one case (fig. 14d), the overpressure associated with the tail wave shock was equal to, or greater than, any of the positive peaks in the signature with a maximum of 6.0 lbs/ft^2 observed on pass 3 of the third flight (fig. 14f).

A summary of the maximum positive overpressures associated with each of the six signatures, as measured by gages 1 and 2, are listed on the right hand side of Table VI along with the signature length (X) and period (ΔT). On the left hand side of the Table are listed the aircraft flight conditions and slant range distance (r) from the probe aircraft perpendicular to the XB-70 flight path. Also shown on the last column on the right of the Table is the calculated maximum overpressure obtained by the “Carlson” method (ref. 18) which was in use at NASA Langley during the time

period of the probe tests. It can be seen from Table VI that good correlation exists between the measured and predicted overpressure levels.

Signature lengths. - The signature lengths X described as the distance between the bow and tail shocks of each of the six probe signatures (listed in Table VI) is based upon the film time interval data of figures 11 to 13 and the aircraft velocities obtained from radar. These values (with the exception of the probe flight of November 23, 1966) along with the average signature length of three XB-70 flights obtained by the cruciform and site 9 ground measurements (see Table VII) are plotted as a function of slant range distance from the XB-70 aircraft and presented in figure 15. Also shown on the figure is a horizontal dashed line representing the length (189 ft.) of the XB-70 generating airplane. The solid line curve represents the calculated values of X from equation (3) of reference 1, which is based upon the far-field volume theory of reference 20 and was in use at the time of these flight experiments.

Both the simplified volume theory and the data points indicate an increasing wavelength with increasing distance from the generating airplane similar to that observed in reference 21 for small projectiles and in figure 12 of reference 22 for two fighter-type aircraft and a bomber aircraft. It is interesting to note the results presented in figure 12 of reference 22 reflect very good correlation with the ground measured signature lengths and those calculated from equation (3) of reference 19 for small aircraft, such as the 54-foot long F-104 and the 65-foot long F8U3. For the 97-foot long B-58, the wavelengths shown in figure 12 of reference 22 obtained from the probe flights (fig. 17 of ref. 9) and ground measurements (ref. 1), the correlation with the simple volume theory begins to deteriorate. This is because the theory assumed volume effects only (no lift effects) and that the aircraft is a point source. In the present case, where the XB-70 length is 189-feet and the effects of lift are quite pronounced as compared to the smaller and lighter weight fighter aircraft, the volume theory curve shown in figure 15 is totally inappropriate.

Ground Measurements

Microphone set-up and characteristics. - Within about 2 to 5 minutes after the completion of the F-104 probe flights, the XB-70 arrived overhead of the main test area (the elevation of EAFB is about 2300 feet above sea level) maintaining essentially the same steady-level flight conditions of about Mach 1.5 at 37,000 feet MSL (see fig. 9a). Two sonic boom ground measurement set-ups were located along the 245 degrees magnetic ground track and consisted of the free-field microphone cruciform array and the Site 9 microphone ground array some 1800 feet up-track (see fig. 9b). The cruciform array consisted of 5 microphones located at ground level at 100-foot separating distance. An additional mast microphone was suspended at a distance of 20 feet directly above the control ground microphone. This array was employed to provide information about the wave shapes, wave angles ϕ, overpressures, durations (periods) and rise times. Aircraft ground speeds were calculated, as were the wave angles in both the horizontal and vertical planes, based on measured shock arrival times. Site 9 involved a ground array of 42 microphones at spacings of 10 to 200 feet in order to assess the influence of the atmosphere on sonic boom waveforms.

Each channel of the measuring system used in ground measurements consisted of a specially modified microphone, tuning unit, d.c. amplifier, oscillograph recorder and FM magnetic tape recorder. The usable frequency range of the complete system, including data reduction, was 0.02

Hz to 5000 Hz. Field calibrations by means of discrete frequency calibrations provided a system accuracy of $\pm$ 1 dB (see ref. 1)

Wave shapes. - Measured sonic boom signatures for the three XB-70 probe flights, as observed at microphone 1 (MLC 1) in the cruciform array and at microphones FRC 1 and LAC 31 in the Site 9 array are shown in figure 16. It may be noted that all eight signatures consisted of three shocks and included a bow and tail shock and an intermediate shock; the signature had not coalesced into a classical N-wave. Bow-shock overpressures ranged from Δp = 2.3 lbs/ft^2 to 3.14 lbs/ft^2 for signatures that are slightly rounded and peaked, respectively. Wave period ranged from 224 ms to 240 ms. Comparison of all eight signatures showed some influence of the atmosphere effects regarding peaking and rounding of the shock fronts.

Signature characteristics. - A summary of the XB-70 sonic boom signature characteristics measured at ground level with the six microphone cruciform array is give in Table VII based on the data taken from reference 23. Signature characteristics included positive and negative overpressures, bow shock rise time to the one-half and maximum amplitudes, wave period and signature length as described in the signature sketches in figure 17. The signature length is obtained from the measured signature period and measured airplane ground speed from the cruciform array. Also listed on the left hand side of the Table are the XB-70 operating conditions of Mach number, altitude, heading, distance lateral to array and boom time. On the right hand side are the shock wave angle, ground speed and the waveform category. The 10-waveform categories used to classify all of the sonic boom signatures acquired during the 1966-67 EAFB National Sonic Evaluation Program (ref. 17) and previous sonic boom flight experiments are also illustrated in figure 17. In addition to the 10 waveform categories shown, word descriptions are also given to each of the categories by means of a single, two, or three letter designation; for instance, a type NP was judged to be intermediate between a type N normal waveform and a type P peaked waveform. An SPR is a spiked-peaked-rounded signature.

Although actual signature traces are no longer available for five of the six cruciform microphones, an examination of the signature characteristics listed in Table VII suggests that the signatures would be very similar to those previously shown (see fig. 16). Note that the free-air microphone (MLC 6) atop the 20-foot mast has a bow-shock overpressure about half that measured at ground level. Also, the signature length X, based on a measured average ground shock speed for the three flights of about 1375 ft/sec and an average wave period of about 232 ms is 320 feet.

Correlation With Airplane Geometry

One of the main objectives of the XB-70/F-104 was the same as for the B-58/F-106 probe tests of reference 9; namely, to obtain definite information relative to the way in which lift effects and volume effects of the much larger and heavier airplane combine in the generation of the shock wave patterns from the generating airplane. The data of figure 18 have been reproduced from figures 11, 12, and 13 to illustrate some of these findings. It was found in references 5 through 9 and reference 11 that the shock wave patterns about an airplane were closely related to the airplane geometry. In the present study, pressure signatures measured above and below the XB-70 generating airplane have been adjusted in signature length to conform to the length of the airplane and are compared with sketches showing the main components of the airplane.

Two general observations can be made. Some correlation exists between the locations of the individual shock waves and the geometrical features of the airplane. It is also obvious that the pressure signatures measured above and to the side of the airplane varies markedly from that measured below the airplane. In particular, the location, number and amplitude of the individual shock waves are different, and furthermore, below the airplane the positive area of the signature exceeds the negative area, whereas the reverse is true above the airplane. Such a result would be expected for airplane operating conditions in which lift effects are significant.

Although the probe measurement that was made at about 3000 feet above the XB-70 was not directly overhead but some 7000 feet to the side, the signature takes on significance relative to defining the initial conditions for the "over-the-top" or "secondary" sonic boom (ref. 14) of which little was known and few were aware of at the time that these tests were conducted.

SUMMARY REMARKS

A series of in-flight flow-field measurements have been made above and below the USAF XB-70-1 airplane using an instrumented NASA F-104 aircraft with a specially designed nose probe. These flight tests were accomplished during the 1966-1967 EAFB National Sonic Boom Evaluation Program and involved three steady-level flights of the XB-70 on three separate days. On all three flights, the XB-70 was at a Mach number of about 1.5 at an altitude of about 37,000 feet above sea level and at gross weights of about 350,000 pounds. A total of six supersonic passes with the F-104 probe aircraft were made through the XB-70 flow field; one above the XB-70 on the first flight, two below the XB-70 on the second flight, and three below the XB-70 on the third flight. Separation distances ranged from about 3000 feet above and 7000 feet (42 body lengths) to the side of the XB-70 and about 2000 feet and 5000 feet (10 to 26 body lengths) below the XB-70. Measured sonic boom signatures from the three XB-70 flights were also acquired at ground level very soon after the probe measurements were acquired (190 body lengths).

The in-flight pressure signatures measured above and below the XB-70 were complex in nature and had the appearance of a "sawtooth" waveform. As many as five major shocks were observed below and near the XB-70 and the number of shocks diminished as distance from the aircraft is increased. The influence of combined lift and volume effects are quite evident when comparing the signatures measured below the aircraft to the one measured above the aircraft. A maximum positive overpressure of about 1.2 lbs/ft^2 was measured above the XB-70 on the first flight (42 body lengths distance), about 2.7 lbs/ft^2 to 5.0 lbs/ft^2 were measured below the XB-70 on the second flight (26 body lengths), and from 3.5 lbs/ft^2 to 5.0 lbs/ft^2 were measured below the XB-70 on the third flight (19 to 10 body lengths). At ground level, the sonic boom signature had not yet coalesced into the classical far-field N-wave but contained an intermediate shock. The maximum bow shock overpressure was about 2.6 lbs/ft^2 and the period of the signature was about 230 msec.

APPENDIX A
(Taken from NASA TN-D 1968, October 1963)

DESCRIPTION AND STATIC CALIBRATION OF PRESSURE INSTRUMENTATION

by John F. Bryant, Jr.

The instrumentation for measuring the pressure field about the bomber airplane consists of the following components: Two NASA model 49-TP inductance pressure gages (ref. 17) and a resistance-type temperature pickup mounted in the special probe on the fighter airplane as shown in figure 5; a carrier amplifier, an NASA recording oscillograph, a resistance-type temperature control box, and an NASA timer mounted in the rocket bay of the fighter airplane; and two solenoid valves and two constant-temperature chambers mounted in the nose bay. The pressure gage converts the static pressure on the probe into impedance changes which produce an unbalance on the inductance-resistance bridge. This output is amplified and demodulated in the carrier amplifier and recorded on film in the oscillograph.

The instrumentation necessary to measure this pressure field had to be suitable for flight environments. Also required was a high sensitivity and a frequency response that was flat from zero to 30 cps. To obtain the high sensitivity, a differential pressure gage was used. An absolute pressure gage, normally used to measure static-pressure changes, would not produce the required high sensitivity. When using a differential gage for this type of measurement, it is necessary to equalize the pressure on the gage during the time that the fighter airplane is climbing and descending. During the measuring period one side of the gage must be sealed off and used as a reference; this was accomplished by connecting one side of the gage to the reference orifice through a solenoid valve. Also connected in the reference side was a constant-temperature chamber. This added volume minimized changes in the reference pressure due to temperature changes caused by the aerodynamic heating of the long lengths of tubing that connected the reference orifice on the instrumented probe with the valve in the nose section. The volume of the tubing was about 1 percent of the chamber volume. To obtain the required frequency response, it was necessary to minimize the time lags by locating the measuring pressure gage very close to the orifice. The NASA type 49 gage was selected because of its high sensitivity, good accelerating characteristics, and very small size. Since its dimensions are only 1/4 by 7/16 inch, the gage could be mounted directly in the probe close to the orifice. All the other instrumentation was standard flight equipment.

It was decided to use two gages: gage 1, which measured the static pressure on the needle nose of the instrumented probe, and gage 2, which measured the static pressure on the body of the probe. (See figs. 4 and 5.) Gage 1 had a sensitivity of approximately 10 lb/sq ft per inch of film deflection and was recorded by a 100-cycle galvanometer. Gage 2 ad a sensitivity of approximately 20 lb/sq ft per inch of film deflection and was recorded by a 50-cycle galvanometer. Once the reference valves are closed, the gages essentially become very sensitive altimeters. Gage 2 was used as a backup in case gage 1 was driven off scale by too large a change in altitude of the fighter airplane after the pilot had closed the reference valve. The lower frequency galvanometer was used to filter out any high-frequency noise that might occur.

The response of each measuring system was determined by the frequency response of the recording galvanometer. An example of this is shown in figure 19, where a step function was applied to the 50-cycle galvanometer and a step function was applied to the entire measuring system. It can be seen from these step functions that the response of both is the same. The time lag of the reference system was 3 seconds. This large lag limited the rate of climb and descent of the fighter airplane to 6,000 feet per minute and thus kept the gages and amplifiers from being overloaded.

The accuracy of the overall system was estimated to be 3 percent of the peak positive overpressures listed in table III. The hysteresis of the gage was 1 percent, and the accuracy of the galvanometers and amplifiers was 2 percent. The change in sensitivity of the gage was 6.5 percent per 100^{o} F change in temperature. This was correctable to 1 percent by use of the resistance temperature gage. The effect of accelerating forces along the longitudinal axis of the fighter airplane (normal to the diaphragm) was 0.05 lb/sq ft per g. The system was constantly monitored by making static calibrations before and after each flight.

APPENDIX B

DESIGN AND AERODYNAMIC CALIBRATION OF PRESSURE PROBE

By Virgil S. Ritchie

DESIGN

Basic Considerations

The design of a flight probe for sensing static-pressure changes in the pressure field of a large disturbance-generating supersonic airplane involved in a number of aerodynamic and structural considerations. A probe of conical shape and relatively large dimensions was considered suitable for a cantilever-type installation at the end of the nose boom of a probe airplane. The conical shape afforded the advantageous features of weak tip disturbance and thin boundary layer. The large dimensions afforded structural rigidity, suitable locations for miniature electrical pressure gages near the pressure-sensing orifices, and relatively large Reynolds numbers. The location of pressure gages near the sensing orifices reduced the possibility of pressure-lag errors. The large Reynolds numbers increased the likelihood of realizing a turbulent boundary layer on the probe without the use of artificial transition-fixing devices, which could introduce shock waves ahead of the pressure-sensing orifices. An arrangement of two small orifices circumferentially located in null-pressure regions about 75° apart afforded some reduction of the errors associated with changes of flow angularity (crossflow) around the conical probe. This asymmetric arrangement necessitated probe orientations with the pressure orifices facing the incident disturbance wave to be measured, but it was considered superior to a symmetrical arrangement of orifices distributed around the circumference of the probe. The asymmetric arrangement was employed for a primary system of pressure orifices located in the conical tip portion of the probe and for a secondary system of orifices located in an enlarged conical region of the probe. For the latter system of orifices, which was employed to supplement the primary systems, suitable calibration information was required, because of likely effects of the probe-enlargement shock wave as well as the thicker boundary layer at the secondary location.

Present Application

Principal details of the flight probe and its installation on the nose boom of a "century series" supersonic airplane are shown in figures 4 and 5. This probe employed six pressure-sensing systems including the two systems for indicating disturbance-related pressure changes, two systems for providing reference pressures for the differential-pressure gages, and systems for providing approximate free-stream static (ambient) pressure and pitot pressure for the airplane flight instruments. The orifices and the tube for providing approximate ambient and pitot pressures for the flight instruments were located at the bottom of the probe for all flights. The forward end of the probe was made rotatable in order to facilitate the required orientation with disturbance-sensing orifices facing the incident disturbance waves from the generating airplane. The rear portion of the probe was secured to the nose boom in such a manner that the angle of attack of the probe would be near 0° for the expected flight conditions. The miniature pressure gages in the probe

were installed with their diaphragms perpendicular to the longitudinal axis of the probe in order to minimize possible effects of lateral acceleration.

WIND-TUNNEL TESTS

Introduction

Early evidence concerning the reflection characteristics of the probe was obtained from unreported preliminary tests of a 0.75-scale model of the flight probe in the Langley 4- by 4-foot supersonic pressure tunnel at a Mach number of about 1.82. The average test Reynolds number (per foot) was about 2.6×10^6, and the average static pressure corresponded to a pressure altitude of about 50,000 feet for standard atmospheric conditions. These tests involved the streamwise movement of the probe (with natural transition) across a disturbance (bow wave) generated by a body of revolution and the measurement of probe-sensed pressure changes in the vicinity of the disturbance. These early tests indicated that the primary system of orifices of the probe sensed the same maximum pressure changes (across the employed shock wave) that were estimated by theoretical methods, whereas the secondary system of orifices sensed pressure changes about 10 percent larger than the estimated values. Also, the probe-sensed pressure changes in the vicinity of the disturbance appeared to be of the type generally associated with turbulent boundary layers (ref. 18). On the basis of this early information, the full-scale flight probe was constructed and the in-flight measurements were undertaken with the view of investigating the reflection characteristics of the flight probe by means of wind-tunnel tests at a later date.

Accordingly, after in-flight measurements, tests of the flight probe were conducted in the Langley 4- by 4-foot supersonic pressure tunnel to calibrate the approximate reflection characteristics of the probe at a Mach number near those employed for the in-flight measurements. The probe reflection characteristics were largely determined by the same procedure as that employed for the early tests at a Mach number of 1.82. This procedure involved streamwise movement of the probe across a weak axisymmetrical shock wave of predetermined strength and the measurement of probe-indicated pressure changes across the disturbance.

Unreported additional tests of the full-scale probe across weak shock waves in the Langley 4- by 4-foot supersonic pressure tunnel provided information concerning the effects of angle of attack on probe reflection characteristics. Although tests have not been included in the present report, the results were used in arriving at the approximate reflection factors reported subsequently in this appendix.

Symbols

M_∞ free-stream Mach number

p_1 static pressure sensed by primary system of orifices (location 1), lb/sq ft

p_2 static pressure sensed by secondary system orifices (location 2), lb/sq ft.

p_3 static pressure sensed by system of orifices (location 3) providing static pressure for probe-airplane flight instruments, lb/sq ft

$p_{1,ref}$ static pressure sensed by orifices providing reference pressure for gage 1, lb/sq ft

$p_{2,ref}$ static pressure sensed by orifices providing reference pressure for gage 2, lb/sq ft

p_t total pressure, lb/sq ft

p_t' pitot pressure, lb/sq ft

p_∞ free-stream static pressure, lb/sq ft

Δp peak or maximum pressure change across oblique shock, lb/sq ft

r radius of body of revolution, in.

x axial distance from nose of body revolution, in.

x_s approximate longitudinal (streamwise) distance from mean location of oblique shock (bow wave), positive when orifices are rearward of shock, in.

y approximate separation distance (perpendicular to airflow direction) between disturbance-generating body and pressure-sensing probe or instrument, in.

α angle of attack of probe, deg

Apparatus and Tests

Test facility and conditions.- The present calibration tests were conducted in the Langley 4- by 4-foot supersonic pressure tunnel at a Mach number of about 2.01 (slightly larger than the average probe-airplane Mach number of about 1.95 employed for in-flight measurements). The average Reynolds number per foot for these tests was about 2.4 x 10^6, whereas the Reynolds numbers per foot for in-flight measurements ranged from about 1.8 x 10^6 to 4.5 x 10^6. The free-stream static pressure employed for the tests corresponded to a pressure altitude about 55,000 feet for standard atmospheric conditions.

Test apparatus and procedures.- The arrangement illustrated at the top of figure 20 was used in the calibration of the flight probe at various angles of attack. This arrangement, involving the location of all static-pressure orifices and the pitot-pressure tube on the bottom of the probe, corresponded to that employed for the probe-airplane flights over the generating airplane. Conical tip 1 (see fig. 5) was used on the probe for the calibrations tests.

The apparatus and arrangements for generating an oblique shock wave and for surveys to determine the strength of this shock are illustrated in figure 21. The procedure employed for surveys in the vicinity of the shock was to move the survey instrument in the streamwise direction and measure the pressures at sufficiently close intervals to define the maximum change of pressure across the shock. Two different methods, one involving a pitot-tube technique and the other a static-pressure orifice on a plate, gave identical results in defining the maximum pressure changes. This oblique shock wave of predetermined strength afforded a means for determining the reflection characteristics of the probe.

Measurements.- Absolute manometers were used for measuring tunnel total pressures as well as reference static pressures and pitot pressures in the test section. Differential-pressure gages with ranges of 0.25 and 0.5 pound per square foot were employed for measuring differences between the reference static pressure and the various local static pressures sensed by the probe or the survey instrument. A gage with a range of 1 pound per square foot was used for measuring differences between the reference pitot pressure and local pitot pressures sensed by the survey instrument. Gages with ranges of 3 and 9 pounds per square foot were used for measuring differences between the total pressure in the tunnel and the pitot pressure sensed by the flight probe. All gages were calibrated before and after the wind-tunnel tests.

Data and Precision

Probe calibration.- Most of the calibration data shown in figure 20 represent averages of measurements from two separate tests. The static-pressure data are expressed in the form of ratios of local probe-sensed static pressures to local free-stream static pressures in order to minimize possible errors associated with flow nonuniformities. Random errors in measurements during probe-calibration and tunnel-calibration tests are believed to influence the static-pressure ratios, as well as the ratios of pitot to total pressure, by no more than ± 0.005.

Pressure measurements in vicinity of oblique shock wave.- Probe-indicated static pressures in the vicinity of the body-generated oblique shock (bow wave) are expressed as ratios of probe-indicated static pressure to an average (not local) free-stream static pressure. Although these ratios are influenced by random errors in measurements in the same manner as the probe-calibration data, the possible errors in measuring pressure changes across the oblique shock wave are considerably less than ± 0.005. The survey technique appears to reduce random errors in measurement to less than about 0.15 percent of the free-stream static pressure or to less than about 3.5 percent of average pressure changes across the shock wave. An experimental measurement-repeatability check, involving several traverses of the probe across the oblique shock wave, indicated scatter of less than ± 2 percent in the shock-wave pressure changes sensed by the primary orifices or by the secondary orifices.

Results and Discussion

Probe calibration at angles of attack.- Calibration tests of the probe at various angles of attack yielded the results shown in figure 20. The primary system of orifices and the reference-pressure orifices in the conical tip portion of the probe indicated pressures which were generally about 1 percent larger than the free-stream static pressure. These cone-surface pressures were sufficiently

influenced by angle-of-attack changes to make the primary pressure-sensing arrangement fairly sensitive to small changes in crossflow such as might be introduced by turbulence, probe oscillations, and flow-angularity changes across shock waves, that might occur in flight. The sensitivity of alternate conical tip 2 to angle-of-attack effects was not determined from calibration tests, but the slightly different circumferential spacings of orifices in tips 1 and 2 (fig. 5) suggest that angle-of-attack effects might be somewhat larger for tip 2 than for tip 1.

The secondary system of orifices and the reference-pressure orifices located in the conical portion of the probe behind the enlargement region indicated pressures 2 or 3 percent less than free-stream static pressure. These pressures were not influenced as much by angle-of-attack changes as were the pressures sensed by the two systems of orifices in the conical tip of the probe.

The orifice system for the flight instruments indicated pressures about 1 or 2 percent less than free-stream static pressure. These pressures were influenced more by angle-of-attack changes than were the pressures indicated by the other orifice systems. This increased influence of angle of attack was largely associated with the size and location of the orifices for the flight-instrument system.

The pitot pressures sensed by the tube that was offset from the bottom of the probe were somewhat larger than those expected for a tube located ahead of the interference field of the probe. The probe-indicated pitot pressures varied consistently with angle-of-attack changes.

Probe capability for sensing pressure changes across an oblique shock wave.- Figure 22(a) illustrates the approximate capability of the probe, at an angle of attack of 0°, for sensing pressures in the vicinity of a weak shock wave. It is seen that the primary system of orifices in the conical tip senses such pressure changes with small error, whereas the secondary system of orifices senses pressure changes considerably larger than the estimated changes. These indicated probe capabilities are supplemented by the data in figure 22(b), which compares probe-indicated, survey-indicated, and estimated maximum pressure changes across the oblique shock wave.

Correlation of these indicated characteristics of the flight probe at an angle of attack of 0° and a Mach number of 2.01 with unreported characteristics of a 0.75-scale model of the flight probe at an angle of attack of 0° and a Mach number of 1.82 indicated that the primary system of orifices is capable of accurately sensing maximum or peak pressure changes across weak shock waves at these Mach numbers. This correlation also indicated that the secondary system of orifices sensed pressure rises that were too large by about 10 percent at a Mach number of 1.82 and about 30 percent at a Mach number of 2.01.

Unreported tests of the flight probe in the vicinity of an oblique shock wave at a Mach number of 2.01 indicated that reflection characteristics of the probe at angles of attack of 1° and -1° were somewhat different from those at an angle of attack of 0°. Such differences were larger for the secondary system or orifices than for the primary system.

The described probe capabilities, as obtained from wind-tunnel tests, are believed to be representative of in-flight probe capabilities at comparable Mach numbers, Reynolds numbers, and

angles of attack. Possible differences in turbulence and boundary-layer transition are believed to be the principal sources of any discrepancies between probe characteristics in the wind tunnel and in flight.

Probe reflection factors for correcting in-flight measurements.- On the basis of the available information, a reflection factor of 1.00 appeared to be appropriate for the primary system of orifices at Mach numbers near 1.82 and 2.01 and angles of attack near 0^o. The reported probe-airplane Mach numbers employed for in-flight measurements were between 1.85 and 1.99. The estimated probe angles of attack for in-flight measurements ranged from -0.4^o to -1.5^o (not including likely changes as the probe airplane traversed the disturbance field of the generating airplane). These negative angles of attack could possibly change the reflection factor by several percent. Angle-of-attack corrections have not been applied to the in-flight pressure measurements obtained from the primary system of orifices.

Reflection factors for the secondary system of orifices appeared to vary with Mach number, probe angle of attack, and strength of the incident disturbance wave. Applicable reflection factors for in-flight measurements obtained from the secondary system of orifices could not be accurately determined from the available information, but the following values are believed to be reliable within about 10 percent:

Flight	Approximate reflection factor for secondary system
1	1.23
2	1.16
3	1.15
4	1.07
5	1.12
6	1.17
7	1.13

The reported values of in-flight pressure data were obtained by dividing the actual measurements by these reflection factors.

General comments.- The supersonic wind-tunnel tests of the probe designed for in-flight measurements yielded the following indications of probe capability for sensing pressure changes across weak disturbances:

(1) The primary system of orifices located in the conical tip portion of the probe appeared to be capable of accurately sensing the maximum or peak changes of static pressure across weak shock waves at Mach numbers near 1.82 and 2.01 when the probe axis was alined with the direction of flight or relative free-stream airflow ($\alpha = 0^o$). The reflection characteristic of the probe were influenced somewhat by small changes in angle of attack.

(2) The secondary system of orifices located in an enlarged conical portion of the probe indicated shock-proximity pressure changes somewhat larger than those obtained by special surveys and by theoretical estimates. Approximate reflection factors for the conditions of the in-flight measurements varied from about 1.07 to about 1.23.

REFERENCES

1. Hubbard, H. H.; Maglieri, D. J.; Huckel, V.; and Hilton, D. A.: Ground Measurements of Sonic Boom Pressures for the Altitude Range of 10,000 to 75,000 Feet. NASA TR R-198, 1964.

2. Maglieri, Domenic J.; Huckel, Vera; and Henderson R.: Sonic Boom Measurements for SR-71 Aircraft Operating at Mach Numbers to 3.0 and Altitudes to 24,384 meters. NASA TN D-6823, 1972.

3. Lee, R. A.; and Downing, J. M.: Sonic Booms Produced by United States Air Force and United State Navy Aircraft: Measured Data, AL-TR-1991-0099, Wright Patterson AFB, Ohio, 1990.

4. Maglieri, Domenic J.: Sonic Boom Flight Research, Some Effects of Airplane Operations and the Atmosphere on Sonic Boom Signatures. NASA SP-147, 1967, pp. 25-48.

5. Maglieri, Domenic J.; Huckel, Vera; and Parrott, Tony L.: Ground Measurements of Shock-Wave Pressure for Fighter Airplanes Flying at Very Low Altitudes and Comments on Associated Response Phenomena. NASA TN D-3443, 1966. (Supersedes NASA TM X-611).

6. Nixon, C. W.; Hill, H. K.; Sommer, N. C.; and Guild, Elizabeth: Sonic Booms Resulting From Extremely Low-Altitude Supersonic Flight: Measurements and Observations on Houses, Livestock and People. AMRL-TR-68-52, U.S. Air Force, 1968.

7. Mullins, Marshall E.: A Flight Test Investigation of the Sonic Boom. AFFTC TN 56-20, Air Res. and Devel, Command, U.S. Air Force, May 1956.

8. Smith, Harriet J.: Experimental and Calculated Flow Fields Produced by Airplanes Flying at Supersonic Speeds. NASA TN D-621, 1960.

9. Maglieri, Domenic J.; Ritchie, Virgil S.; and Bryant, John F., Jr.: In-Flight Shock Wave Pressure Measurements Above and Below a Bomber Airplane at Mach Numbers from 1.42 to 1.69. NASA TN D-1968, 1963.

10. Maglieri, Domenic J.; Huckel, V.; Henderson, H. R.; and Putnam, T.: Preliminary Results of XB-70 Sonic Boom Field Tests During National Sonic Boom Evaluation Program. NSBEO 1-67, pp C-II to C-II-17, July 28, 1967.

11. Haering, Edward A.; Jr.; Ehernberger, L. J.; and Whitmore, Stephen A.: Preliminary Airborne Measurement for the SR-71 Propagation Experiment. NASA TM-104307, 1995.

12. Tinetti, Ana F.; Maglieri, Domenic J.; Driver, Cornelius; and Bobbitt, Percy J.: Equivalent Longitudinal Area Distributions of the B-58 and XB-70-1 Airplanes for Use in Wave Drag and Sonic Boom Calculations. NASA/CR-2011-217078, 2011.

13. Garrick, I. E.; and Maglieri, D. J.: A Summary of Results on Sonic Boom Pressure Signature Variations Associated with Atmospheric Conditions, NASA TN-D 4588, 1968.

14. Maglieri, Domenic J.; Carlson, Harry W.; and Hubbard, Harvey H.: Status of Knowledge of Sonic Booms. Noise Control Eng. Vol. 15, No. 2, Sept.-Oct. 1980, pp. 57-64.

15. Powers, John O.; Sands, J. M.; and Maglieri, Domenic J.: Survey of U.S. Sonic Boom Overflight Experimentation. AGARD Conference Proceedings No. 42, "Aircraft Engine Noise and Sonic Boom," May 1969.

16. Arnaiz, Henry H.; Peterson, John B., Jr.; Daugherty, James C.: Wind-Tunnel Flight Correlation Study of Aerodynamic Characteristics of a Large Flexible Supersonic Cruise (XB-70-1): III - A Comparison Between Characteristics Predicted From Wind-Tunnel Measurements and Those Measured in Flight. NASA TP-1516, 1980.

17. National Sonic Boom Evaluation Office: Sonic Boom Experiments at Edwards Air Force Base, NSBEO-1-67 (Contract AF 49 (638)-1058), Stanford Research Inst., July 28, 1967.

18. Middleton, Wilbur, D.; and Carlson, Harry W.: A Numerical Method for Calculating Near-Field Sonic-Boom Pressure Signatures. NASA TN-D 3082, 1965.

19. Maglieri, Domenic J.; Hubbard, Harvey H.; and Lansing, Donald L.: Ground Measurements of the Shock-Wave Noise From Airplanes in Level Flight at Mach Numbers to 1.4 and at Altitudes to 45,000 Feet. NASA TN D-48, 1959.

20. Whitham, G. B.: The Behavior of Supersonic Flow Past a Body of Revolution, Far From the Axis. Proc. Roy. Soc. (London), ser. A, vol. 201, no. 1064, Mar. 7, 1950, pp. 89-109.

21. DuMond, Jesse W.M.; Cohen, E. Richard; Panofsky, W.K.H.; and Deeds, Edward: A Determination of the Wave Forms and Laws of Propagation and Dissipation of Ballistic Shock Waves. J.Acous. Soc. of America, vol. 18, no. 1, July 1946, pp. 97-118.

22. Maglieri, Domenic J.; Parrott, Tony L.; Hilton, David A.; and Copeland, William L.: Lateral-Spread Sonic-Boom Ground-Pressure Measurements From Airplanes at Altitudes to 75,000 Feet at Mach Numbers to 2.0. NASA TN D-2021, 1963.

23. Hubbard, H. H.; and Maglieri, D. J.: Sonic Boom Signature Data from Cruciform Microphone Array Experiments During the 1966-67 EAFB National Sonic Boom Evaluation Program. NASA CR-182027, 1990.

24. Patterson, John L.: A Miniature Electrical Pressure Gage Utilizing a Stretched Flat Diaphragm. NACA TN 2659, 1952.

25. Liepmann, H. W., Roshko, A., and Dhawan, S.: On Reflection of Shock Waves From Boundary Layers. NASA Rep. 1100, 1952. (Supersedes NACA TN 2334.)

26. Whitham, G. B.: The Flow Pattern of a Supersonic Projectile. Communications on Pure and Appl. Math., vol. V, no. 3, Aug. 1952, pp. 301-348.

27. Carlson, Harry W.: An Investigation of Some Aspects of the Sonic Boom By Means of Wind-Tunnel Measurements of Pressures About Several Bodies at a Mach Number of 2.01. NASA TN D-161, 1959.

Table I.- Geometric characteristics of XB-70-1 airplane.
(from reference 16)

Total wing	
Total area (includes 230.62 m^2 (2482.34 ft^2) covered by fuselage but not 3.12 m^2 (33.53 ft^2) of the wing ramp area), m^2 (ft^2)	585.07 (6297.8)
Span, m (ft)	32 (105)
Aspect ratio	11.751
Taper ratio	0.019
Dihedral angle, deg	0
Root chord (wing station 0), m (ft)	35.89 (117.76)
Tip chord (wing station 16m (630 in.)), m (ft)	0.67 (2.19)
Mean aerodynamic chord (wing station 5.43 m (17.82 (ft)), m (ft)	23.94 (78.532)
Fuselage station of 25-percent wing mean aerodynamic chord, m (ft)	41.18 (135.10)
Sweepback angle, deg:	
Leading edge	65.57
25-percent element	58.79
Trailing edge	0
Incidence angle, deg:	
Root (fuselage juncture)	0
Tip (fold line and outboard	-2.60
Airfoil section (modified hexagonal):	
Root to wing station 4.72m (186 in.) (thickness-chord ratio, 2 percent)	0.30 to 0.70
Wing station 11.68 m (460 in.) to 16.00 m (630 in.) (thickness-chord ratio, 2.5 percent)	0.30 to 0.70
Inboard wing -	
Area (includes 230.62 m^2 (2482.34 ft^2)covered by fuselage but not 3.12 m^2 (33.53 ft^2) wing ram area, m^2 (ft^2)	488.28 (5256.0)
Span, m (ft)	19.34 (63.44)
Aspect ratio	0.766
Taper ratio	0.407
Dihedral angle, deg	0
Root chord (wing station 0), m (ft)	35.89 (117.76)
Tip chord (wing station 9.67 m (380.62 in.)), m (ft)	14.61 (47.94)
Mean aerodynamic chord (wing station 4.15 m (163.58 in.)), m (in.)	26.75 (1053)
Fuselage station of 25-percent wing mean aerodynamic chord, m (in)	39.07 (1538.29)
Sweepback angle, deg:	
Leading edge	65.57
25-percent element	58.79
Trailing edge	0
Airfoil section (modified hexagonal):	
Root (thickness-chord ratio, 2 percent)	0.30 to 0.70
Tip (thickness-chord ratio, 2.4 percent)	0.30 to 0.70

Table I.- Continued.

Mean camber (leading edge), deg:		
Butt plane 0		0.15
Butt plane 2.72 m (107 in.)		4.40
Butt plane 3.89 m (153 in.)		2.75
Butt plane 6.53 m (257 in.)		2.60
Butt plane 9.32 m (367 in.) to tip		0
Outboard wing -		
Area (one side only), m^2 (ft^2)		48.39 (520.90)
Span, m (ft)		6.33 (20.78)
Aspect ratio		0.829
Taper ratio		0.046
Dihedral angle, deg		5
Root chord (wing station 9.67 m) (380.62 in.)), m (ft)		14.61 (47.94)
Tip chord (wing station 16.00 m) (630 in.)), m (ft)		0.67 (2.19)
Mean aerodynamic chord (wing station 11.87 m) (467.37 in.)), m (in.)		9.76 (384.25)
Sweepback angle, deg:		
Leading edge		65.57
25-percent element		58.79
Trailing edge		0
Airfoil section (modified hexagonal):		
Root (thickness-chord ratio, 2.4 percent)		0.30 to 0.70
Tip (thickness-chord ratio, 2.5 percent)		0.30 to 0.70
Down deflection from wing reference plane, deg		0,25,65
Skewline of tip fold, deg:		
Leading edge in		1.5
Leading edge down		3

	Wing tips	
	Up	Down
Elevons (data for one side):		
Total area aft of hinge line, m^2 (ft^2)	18.37 (197.7)	12.57 (135.26)
Span, m (ft)	6.23 (20.44)	4.26 (13.98)
Inboard chord (equivalent), m (in.)	295 (116)	(116) 2.95
Sweepback angle of hinge line, deg	0	0
Deflection, deg:		
As elevator		-25 to 15
As aileron with elevators at $\pm 15^\circ$ or less		−15 to 15
As aileron with elevators at -25° or less		-5 to 5
Total		-30 to 30
Canard -		
Area (includes 13.96 m^2 (150.31 ft^2) covered by fuselage), m^2 (ft^2)		38.61 (415.59)
Span, m (ft)		8.78 (28.81)
Aspect ratio		1.997

Table I.- Continued.

Taper ratio	0.388
Dihedral angle, deg	0
Root chord (canard station 0), m (ft)	6.34 (20.79)
Tip chord (canard station 4.39 m (172.86 in.)), m (ft)	2.46 (8.06)
Mean aerodynamic chord (canard station 1.87 m (73.71 in.)), m (in.)	4.68 (184.3)
Fuselage station of 25-percent canard mean aerodynamic chord, m (in.)	14.06 (553.73)
Sweepback angle, deg:	
leading edge	31.70
25-percent element	21.64
trailing edge	-14.91
Incidence angle (nose up), deg	0 to 6
Airfoil section (modified hexagonal):	
root (thickness-chord ratio 2.5 percent)	0.34 to 0.66
tip (thickness-chord ratio 2.52 percent)	0.34 to 0.66
Ratio of canard area to wing area	0.066
Canard flap (one of two):	
Area (aft of hinge line), m^2 (ft^2)	5.08 (54.69)
Ratio of flap area to canard semiarea	0.263
Vertical tail (one of two) -	
Area (includes 0.83 m^2 (8.96 ft^2) blanketed area), m^2 (ft^2)	21.74 (233.96)
Span, m (ft)	4.75 (15)
Aspect ratio	1
Taper ratio	0.30
Root chord (vertical-tail station 0), m (ft)	7.03 (23.08)
Tip chord (vertical-tail station 4.57 m (180 in.)), m (ft)	211. (6.92)
Mean aerodynamic chord (vertical-tail station 1.88 m (73.85 in.)), m (in.)	5.01 (197.40)
Fuselage station of 25-percent vertical-tail mean aerodynamic chord, m (in.)	55.59 (2188.50)
Sweepback, angle, deg:	
Leading edge	51.77
25-percent element	45
Trailing edge	10.89
Airfoil section (modified hexagonal):	
Root (thickness-chord ratio 3.75 percent)	0.30 to 0.70
Tip (thickness-chord ratio 2.5 percent)	0.30 to 0.70
Cant angle, deg	0
Ratio of vertical tail to wing area	0.037
Rudder travel, deg:	

Table I.- Continued.

With gear extended	±12
With gear retracted	±3
Fuselage (includes canopy) -	
Length, m (ft)	56.62 (185.75)
Maximum depth (fuselage station 22.30 m (878 in.)), M (in.)	2.72 (106.92)
Maximum breadth (fuselage station 21.72 m (855 in.)), m (in.)	2.54 (100)
Side area, m^2 (ft^2)	87.30 (939.72)
Planform area, m^2 (ft^2)	110.07 (1184.78)
Center of gravity:	
Forward limit, percent mean aerodynamic chord	19.0
Aft limit, percent mean aerodynamic chord	25.0
Duct -	
Length, m (ft)	31.96 (104.84)
Maximum depth (fuselage station 34.93 m (1375 in.)), m (in.)	2.31 (90.75)
Maximum breadth (fuselage station 53.34 m (2100 in.)), m (in.)	9.16 (360.70)
Side area, m^2 (ft^2)	66.58 (716.66)
Planform area, m^2 (ft^2)	217.61 (2342.33)
Inlet captive area (each), m^2 (in^2) 3.61 (5600)	3.61 (5600)
Surface areas (net wetted), m^2 (ft^2) -	
Fuselage, canopy, boundary layer gutter, and tailpipes	264.77 (2850.0)
Ducts	318.71 (3430.6)
Wing, wing tips, and wing ramp	864.71 (9307.7)
Vertical tails (two)	87.12 (937.7)
Canard	49.47 (532.5)
Total	1584.79 (17,058.5)
Engines (six)	YJ93-GE-3
Boattail angle, deg -	
Upper surface	6
Lower surface	5
Side	6
Base areas, m^2 (ft^2) -	
Total	12.7 (137)
Total (all engines on, minimum exit area)	10 (107.2)
Total (all engines on, maximum exit area)	4.5 (48.5)
Projected thickness (height) of base, m (in.)	1.47 (58)
Width of propulsion package, cm (in.)	914 (360)
Engine -	
Jet-exit area (minimum), cm^2 (in^2)	4613 (715)

Table I.- Concluded.

Jet-exit area (maximum), cm^2 (in^2)	13,678 (2120)
Jet-exit diameter (minimum), cm (in.)	77 (30.2)
Jet-exit diameter (maximum), cm (in.)	132 (52)

Table II.- Summary of XB-70 and F-104 in-flight probe test conditions.

Date	MSN	Probe run	Flight Condition		Shock Penetration time, (Z)	XB-70 Generating Aircraft								F-104 Probe Aircraft					ΔM	ΔV	Position of F-104 relative to XB-70 (ft)				
			Probing Region	Probing Region		Altitude (ft. msl)	M	Grd. Velocity (ft/sec)	True hdg. (deg)	Gross weight (lb)	Canard pos. (deg)	left hand	right hand	Altitude (ft. msl)	M	Grd. velocity (ft/sec)	V_{104}	True hdg. (deg)		(ft/sec)	S (behind)	Y (to side)	Z (above below)	r (slant range)	r/l
11/23/66	1-1	1	F-104 above XB-70	XB-70 overtakes F-104	18:27:45	36,550	1.45	1360	259	324,000	1.05	11.6	11.4	39,840	1.15	1050	-3	273	.30	310	10,750	7,100	-3,290	7825	42
12/12/66	3-2	1	F-104 below XB-70	XB-70 overtakes F-104	18:27:32	37,639	1.50	1371	261	344,000	1.08	11.5	11.3	32,912	1.32	1216	-2	263	.18	155	5525	220	4727	4732	26
		2		F-104 overtakes XB-70	18:29:18	37,584	1.49	1303	261	340,000	1.07	11.7	10.4	32,928	1.83	1707	+6	261	.34	344	5275	825	4656	4729	26
12/16/66	4-2	1	F-104 below XB-70	XB-70 overtakes F-104	15:52:06	37,870	1.47	1372	261	350,000	1.15	11.4	10.9	36,000	1.18	1104	-4.5	263	.29	268	2850	2900	1870	3451	19
		2		F-104 overtakes XB-70	15:54:06	37,900	1.46	1370	262	348,500	1.14	11.8	11.3	35,869	1.61	1523	-2.5	262	.15	153	2590	980	2031	2257	12
		3		XB-70 overtakes F-104	15:54:04	37,917	1.47	1360	260	344,000	1.10	12.3	11.4	36,115	1.34	1257	-2.04	260	.13	103	2050	590	1802	1896	10

Table III.- XB-70 flight conditions overhead of ground cruciform microphone array.

Date	MSN	Time (Z)	Altitude (ft.msl)	M	Grd. velocity (ft/sec)	Lateral Offset, (n.mi.)	Gross weight, W (lb)	Canard pos. (deg)	Average elevon position (deg)		True heading (deg)
									left hand	right hand	
11/23/66	1-1	18:31:00	37,200	1.46	1342	1.69S	315,000	0.92	13.0	11.9	259
12/12/66	3-2	18:31:00	37,600	1.50	1384	0.17S	339,000	1.00	11.7	10.4	262
12/16/66	4-2	15:57:00	38,600	1.46	1399	0	339,000	1.11	11.9	11.3	262

Table IV. - Upper air atmospheric data.
(a) rawinsondes for November 23, 1966 (launch times PST)

1966 11 23 1200:00						1966 11 23 1800:00					
				Wind						Wind	
Alt m	Press kPa	Temp C	RH %	Dir deg	Speed m/s	Alt m	Press kPa	Temp C	RH %	Dir deg	Speed m/s
724.	93.10	3.0	82	240	1	724.	93.40	8.1	69	0	0
560.	95.00	**	***	***	***	582.	95.00	***	***	***	***
1002.	90.00	5.8	65	255	5	1027.	90.00	4.3	54	34	2
1467.	85.00	2.7	49	225	4	1489.	85.00	1.6	59	40	4
1955.	80.00	-0.1	38	214	4	1976.	80.00	-1.2	63	62	4
2469.	75.00	-1.9	15	332	8	2487.	75.00	-3.8	34	137	1
3014.	70.00	-6.4	18	340	11	3028.	70.00	-7.6	36	239	4
3587.	65.00	-11.5	17	277	8	3600.	65.00	-11.7	40	250	5
4195.	60.00	-15.3	17	280	9	4208.	60.00	-15.7	34	231	10
4848.	55.00	-19.5	17	264	10	4858.	55.00	-20.1	28	223	11
5550.	50.00	-23.3	18	237	18	5562.	50.00	-23.6	23	229	15
6316.	45.00	-27.6	16	228	28	6322.	45.00	.28.8	24	225	21
7152.	40.00	-33.7	15	227	33	7155.	40.00	-34.6	26	223	26
8078.	35.00	-39.3	17	224	38	8077.	35.00	-40.1	26	225	34
9118.	30.00	-45.4	19	223	42	9118.	30.00	-45.1	26	226	41
10318.	25.00	-50.3	20	224	45	10318.	25.00	-50.1	26	224	42
11763.	20.00	-52.6	21	229	38	11768.	20.00	-52.0	25	222	35
12626.	17.50	-53.3	22	231	31	12631.	17.50	-52.7	24	226	29
13614.	15.00	-54.8	20	232	27	13623.	15.00	-53.5	24	227	27
14771.	12.50	-58.9	22	229	27	14789.	12.50	-57.0	25	224	25
16170.	10.00	-59.8	22	225	18	16195.	10.00	-58.7	23	215	16
17567.	8.00	-60.0	22	227	12						
18395.	7.00	-60.2	22	230	9	17598.	8.00	-59.3	22	216	12
19363.	6.00	-60.5	22	232	1	18440.	7.00	-57.9	22	212	9
20501.	5.00	-59.5	22	206	11	19405.	6.00	-59.2	22	171	5
21902.	4.00	-59.9	22	152	4	20550.	5.00	-57.5	22	121	2
23708.	3.00	-56.2	22	78	6	21966.	4.00	-58.2	22	104	3
24845.	2.50	-58.1	22	71	6	23787.	3.00	-55.4	22	74	9
26273.	2.00	-55.1	22	68	8	24946.	2.50	-55.2	22	72	13
28134.	1.50	-51.2	22	75	16	26377.	2.00	-51.0	22	82	13
30787.	1.00	-45.7	22	73	14	28270.	1.50	-45.7	22	70	12
33151.	0.70	-41.3	22	43	14	31014.	1.00	-42.3	22	85	14

Table IV. - Continued

(b) rawinsondes for December 12, 1966 (launch times PST)

1966 12 12 1200:00

Alt	Press	Temp	RH	Wind	
				Dir	Speed
m	kPs	C	%	deg	m/s
724.	94.10	-0.2	83	250	1
646.	95.00	***	***	***	***
1090.	90.00	9.2	61	30	3
1564.	85.00	8.9	35	56	5
2065.	80.00	8.8	12	69	4
2598.	75.00	7.9	10	75	2
3163.	70.00	3.8	14	41	2
3759.	65.00	-1.0	20	336	3
4392.	60.00	-5.9	17	290	5
5066.	55.00	-11.1	10	304	5
5789.	50.00	-16.8	11	303	11
6571.	45.00	-23.1	11	305	10
7421.	40.00	-29.9	11	300	9
8357.	35.00	-37.5	17	291	9
9400.	30.00	-46.4	28	294	15
10584.	25.00	-55.9	38	287	22
11984.	20.00	-60.4	35	270	32
12812.	17.50	-60.4	32	264	29
13779.	15.00	-59.4	26	259	28
14910.	12.50	-62.5	24	257	29
16274.	10.00	-66.7	22	260	24
17614.	8.00	-69.8	22	268	16
18417.	7.00	-67.9	22	274	12
19346.	6.00	-66.3	22	277	7
20457.	5.00	-62.8	22	288	6
21840.	4.00	-60.0	22	313	6
23646.	3.00	-57.2	22	275	8
24795.	2,50	-56.8	22	252	9
26226.	2.00	-55.8	22	250	10

1966 12 12 1800:00

Alt	Press	Temp	RH	Wind	
				Dir	Speed
m	kPa	C	%	deg	m/s
724.	94.20	6.7	68	120	1
651.	95.00	***	***	***	***
1098.	90.00	8.6	52	55	2
1570.	85.00	8.7	31	49	5
2073.	80.00	10.7	13	74	5
2608.	75.00	7.9	14	92	2
3173.	70.00	4.2	16	87	1
3770.	65.00	-0.9	22	278	5
4403.	60.00	-6.1	22	275	6
5076.	55.00	-11.5	18	265	2
5798.	50.00	-17.0	16	300	6
6580.	45.00	-23.3	30	285	12
7430.	40.00	-30.0	36	273	12
8367.	35.00	-37.1	62	264	11
9413.	30.00	-46.1	58	261	15
10595.	25.00	-56.8	55	266	19
11987.	20.00	-61.2	48	276	22
12815.	17.50	-61.3	42	274	22
13769.	15.00	-61.5	34	266	23
14895.	12.50	-62.5	30	258	23
16268.	10.00	-63.9	24	260	19
17622.	8.00	-67.9	22	271	15
18434.	7.00	-64.0	22	274	12
19386.	6.00	-62.8	22	278	8
20514.	5.00	-61.3	22	295	6
21902.	4.00	-59.6	22	290	3
23708.	3.00	-57.3	22	281	9
24849.	2.50	-55.9	22	269	9
26286.	2.00	-55.2	22	254	7
28134.	1.50	-54.3	22	260	12
30712.	1.00	-50.7	22	254	23
33050.	0.70	-40.1	22	***	***

Table IV. - Concluded

(c) rawinsondes for December 16, 1966 (launch times PST)

1966 12 16 0900:00

Alt	Press	Temp	RH	Wind	
				Dir	Speed
m	kPa	C	%	deg	m/s
724.	94.10	1.7	60	0	0
645.	95.00	***	***	***	***
1093.	90.00	10.3	20	59	5
1566.	85.00	8.3	17	73	8
2064.	80.00	6.5	13	86	7
2595.	75.00	7.2	19	126	6
3159.	70.00	3.8	25	127	3
3756.	65.00	0.0	35	148	3
4401.	60.00	-5.7	42	102	4
5085.	55.00	-8.1	15	32	6
5820.	50.00	-12.6	16	352	6
6617.	45.00	-17.8	17	359	2
7484.	40.00	-25.2	19	145	1
8436.	35.00	-34.3	20	235	3
9494.	30.00	-43.1	21	227	8
10695.	25.00	-53.1	23	235	13
12099.	20.00	-62.8	23	229	16
12914.	17.50	-65.9	23	232	14
13846.	15.00	-67.3	23	245	10
14944.	12.50	-69.8	22	253	10
16281.	10.00	-69.7	22	274	7
17614.	8.00	-67.1	22	306	5
18417.	7.00	-67.1	22	321	5
19346.	6.00	-65.2	22	339	4
20465.	5.00	-63.3	22	339	4
21840.	4.00	-60.7	22	296	7
23625.	3.00	-60.4	22	258	7
24770.	2.50	-61.1	22	280	11
26139.	2.00	-58.4	22	273	15
27961.	1.50	-54.7	22	263	26
30636.	1.00	-47.4	22	***	***

1966 12 16 1800:00

Alt	Press	Temp	RH	Wind	
				Dir	Speed
m	kPa	C	%	deg	m/s
724.	94.20	4.7	36	180	1
654.	95.00	***	***	***	***
1100.	90.00	9.2	25	70	2
1572.	85.00	7.2	24	64	4
2069.	80.00	6.3	20	104	4
2600.	75.00	6.9	20	135	3
3163.	70.00	3.3	26	156	3
3759.	65.00	-0.7	32	178	5
4393.	60.00	-5.9	35	190	7
5068.	55.00	-9.0	19	187	7
5802.	50.00	-12.4	16	168	2
6598.	45.00	-18.4	14	185	3
7464.	40.00	-25.4	16	169	7
8417.	35.00	-33.8	18	180	11
9476.	30.00	-43.1	20	206	14
10676.	25.00	-53.0	22	228	19
12086.	20.00	-61.7	23	239	17
12900.	17.50	-67.2	23	233	16
13832.	15.00	-66.8	23	229	16
14939.	12.50	-65.6	22	233	12
16295.	10.00	-64.7	22	258	8
17652.	8.00	-66.7	22	292	5
18460.	7.00	-65.2	22	301	3
19407.	6.00	-63.3	22	300	3
20526.	5.00	-62.6	22	345	4
21902.	4.00	-60.6	22	334	4
23678.	3.00	-58.8	22	293	7
24845.	2.50	-58.0	22	288	13
26273.	2.00	-55.9	22	281	17
28091.	1.50	-54.7	22	279	18
30757.	1.00	-46.9	22	***	***

Table V.- Surface weather observations at EAFB runway 22/04

Test date	Time, Z	Temp, ^{o}F	Wind, deg/kts	Cloud cover	Precipitation
11-23-66	17:56:00	44	000/00	clear	none
	18:56:00	47	000/00	clear	none
12-12-66	17:55:00	42	000/00	overcast	none
	18:55:00	42	110/02	overcast	none
12-16-66	14:57:00	27	310/02	scattered	none
	15:55:00	30	000/00	broken	none

Table VI.- Summary of XB-70 maximum positive overpressures, signature lengths, and periods for in-flight probe tests.

Date	MSN	Probe run	XB-70		F-104	r (ft)	Measured				Calculated
			M	Altitude (ft. MSL)	Altitude (ft. MSL)		Gage 1 ($\Delta p_{,max}$, lbs/sq.ft.)	Gage 2 ($\Delta p_{,max}$, lbs/sq.ft.)	X (ft)	ΔT (msec)	Δp_{max} (lb/sq.ft)
11/23/66	1-1	1	1.45	36,550	39,840	7825	1.02	1.31	529	389	1.05
12/12/66	3-2	1	1.50	37,639	32,912	4732	2.80	2.76	198	144	2.60
		2	1.49	37,584	32,928	4729	2.80	2.27	220	162	
12/16/66	4-2	1	1.47	37,870	36,000	3451	3.40	3.50	252	184	4.40
		2	1.46	37,900	35,869	2257	4.12	-	211	154	
		3	1.47	37,917	36,115	1896	5.10	4.11	188	138	

Table VII.- XB-70 sonic boom signature characteristics measured at ground level with six microphone cruciform array
(Calculated $\Delta P_{max} \sim 2.40$ lb./sq. ft.)

Date	Mission Number	Alt. ft MSL	Mach No.	Head deg mag	Offset (n.mi.)	Boom time (Zulu)	Micro-phone No.	Peak amplitudes, positive (lb/sq.ft.)			Peak Amplitudes Negative (lb/sq.ft)		$\tau_{\frac{1}{2}}$	τ	ΔT	ΔX	Shock Wave angle ϕ	Ground speed	Waveform Category
								P1*	P2*	P3*	P1*	P2*	(msec)	(msec)	(msec)	(ft)	(deg)	(ft/sec)	
11-23-66	1-1	37,200	1.46	243	1.69S	1831:43	MLC1	**	**	3.06	2.29	2.50	0.5	1.5	229	307	58.9	1342	NP
							MLC2	**	**	2.91	2.34	2.67	0.5	6.5	229	307			NP
							MLC3	**	**	2.78	2.22	2.38	0.2	5.0	229	307			NP
							MLC4	**	**	2.86	2.18	2.64	0.6	2.0	230	309			NP
							MLC5	**	**	2.94	2.37	2.84	0.3	3.0	231	310			NP
							MLC6	**		1.44	**	**	**	**	**	**			**
12-12-66	3-2	37,600	1.50	246	0.15S	1831:42	MLC1	**	**	2,57	2.27	2.50	0.3	5.0	234	324	56.7	1384	NP
							MLC2	**	**	2.42	1.79	2.39	0.4	5.0	233	322			NP
							MLC3	**	**	2.39	2.10	2.25	0.3	5.0	234	324			NP
							MLC4	**	**	2.47	2.13	2.51	0.5	4.5	234	324			NP
							MLC5	**	**	2.53	2.23	2.63	0.5	4.0	234	324			NP
							MLC6	**	**	1.30	**	**	**	**	**	**			**
12-16-66	4-2	38,600	1.46	246	0	1557:49	MLC1	**	**	2,57	2.24	2.27	0.2	5.0	232	321	55.0	1399	NP
							MLC2	**	**	2,57	2.32	2.29	0.5	5.0	232	321			NP
							MLC3	**	**	2.49	2.23	2.02	0.5	5.0	232	321			NP
							MLC4	**	**	2.39	2.11	2.29	0.8	6.0	232	321			NP
							MLC5	**	**	2.43	2.12	2.22	0.6	5.0	232	321			NP
							MLC6	**	**	1.17	**	**	**	**	**	**			**

* See figure 7 for definition.

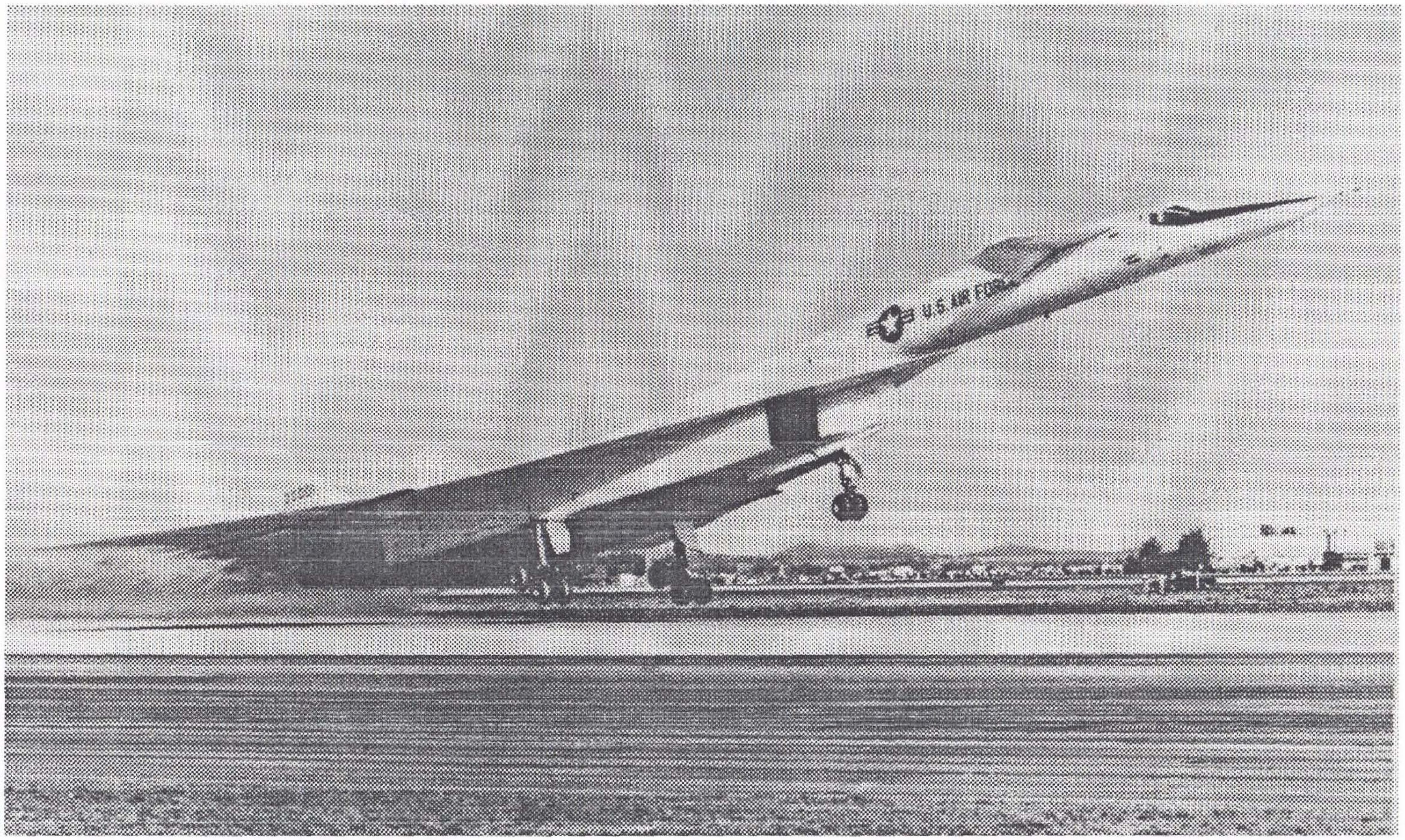

(Courtesy of NASA Flight Research Center)

Figure 1.- Photograph of XB-70-1 delta wing supersonic aircraft used as the sonic boom generator in the present studies.

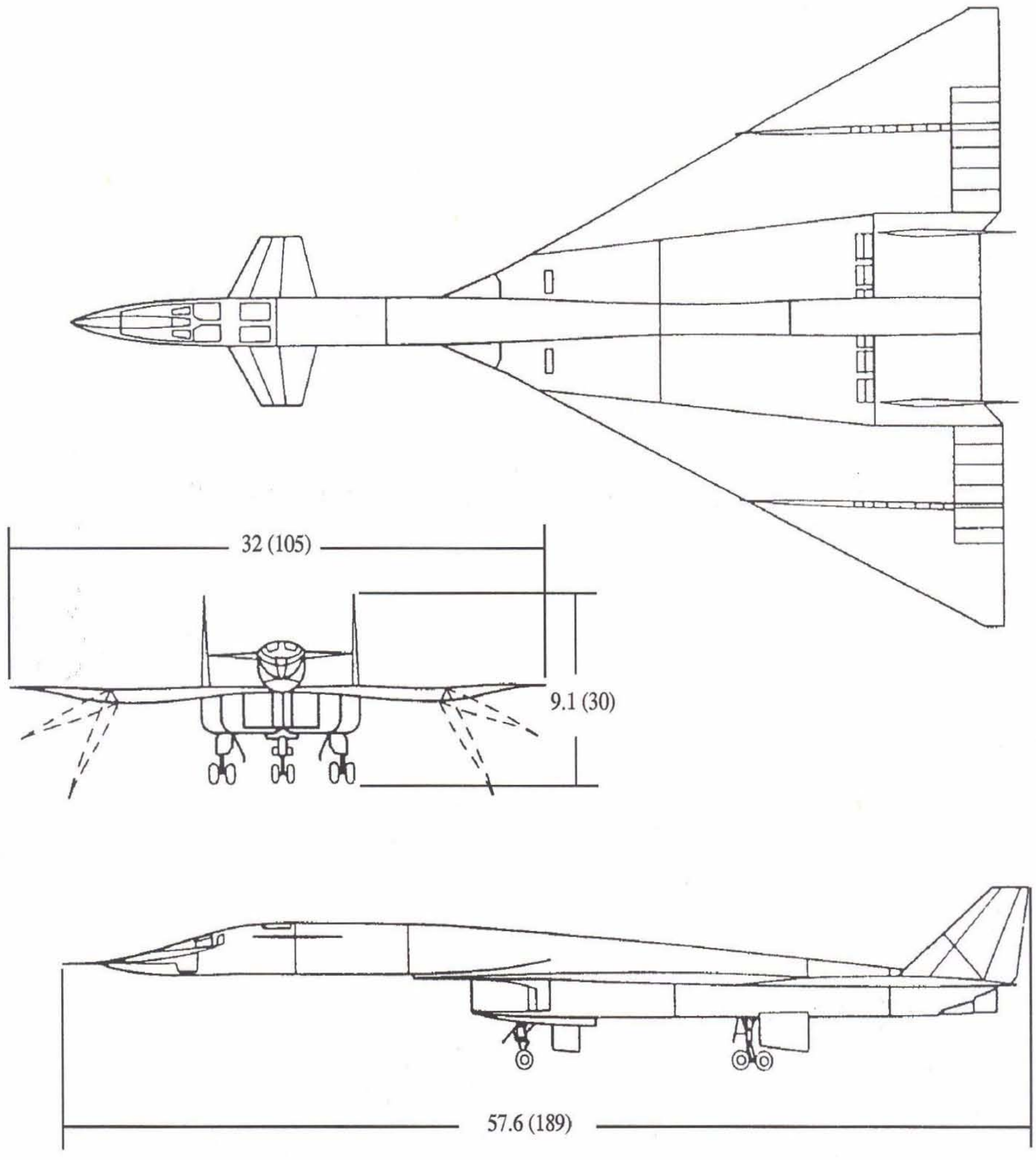

Figure 2.- Three-view drawing of XB-70-1 airplane. Dimensions are in meters (feet). Total wing area is 6297.8 feet (from ref. 16)

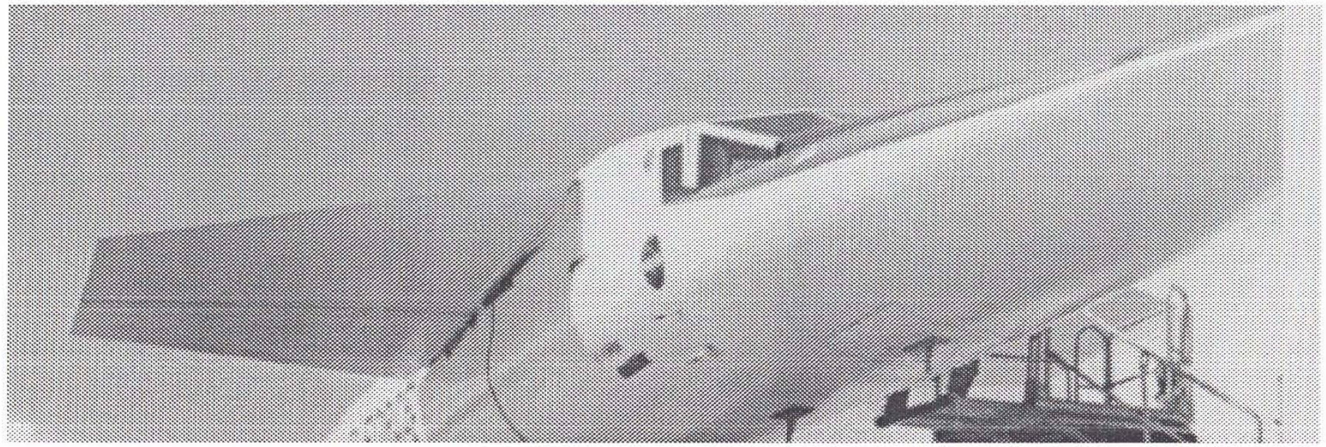

(a) windshield-nose ramp down

(Courtesy of U. S. Air Force)

(b) windshield-nose ramp up

Figure 3.- Photographs of XB-70 showing windshield-nose ramp positions.

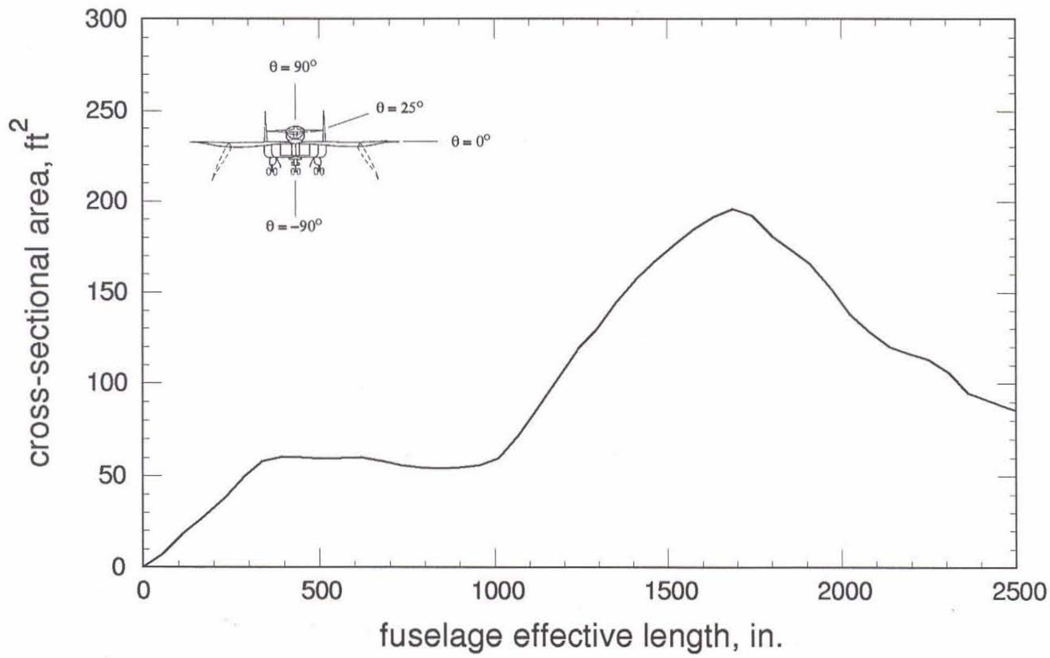

(a) Total area distribution based on oblique cuts for a position above and to the side of the aircraft (θ = 25°)

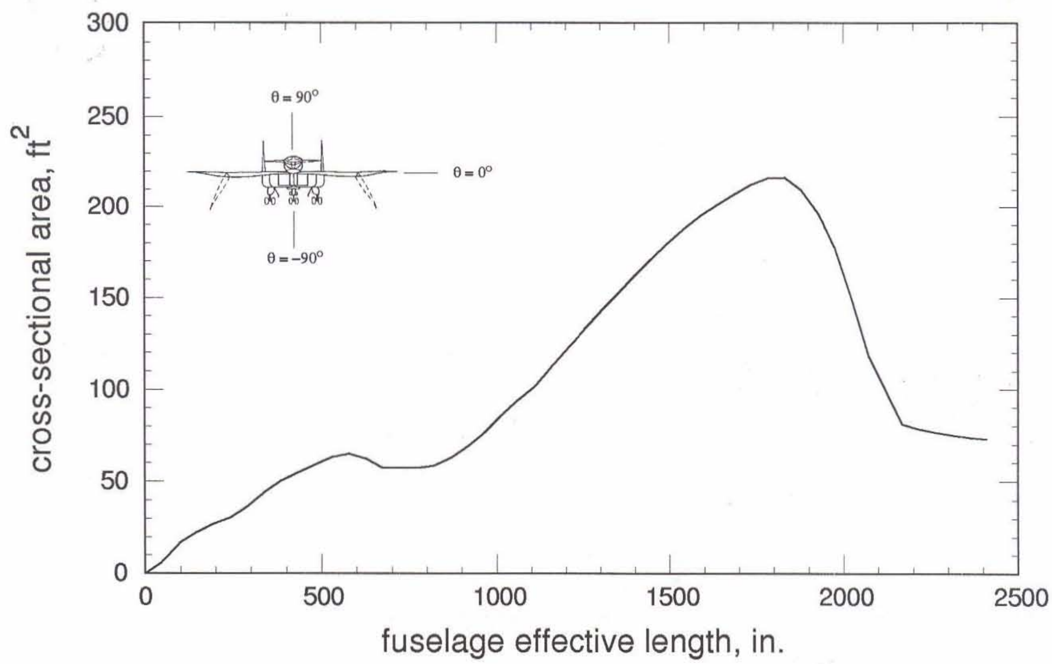

(b) Total area distribution based on oblique cuts for a position below the aircraft (θ = -90°)

Figure 4.- Area distributions of XB-70-1 vehicle used as shock-wave generating airplane. Oblique cuts at Mach 1.5 (inlet capture area not included. Wing tips down at 65° down).

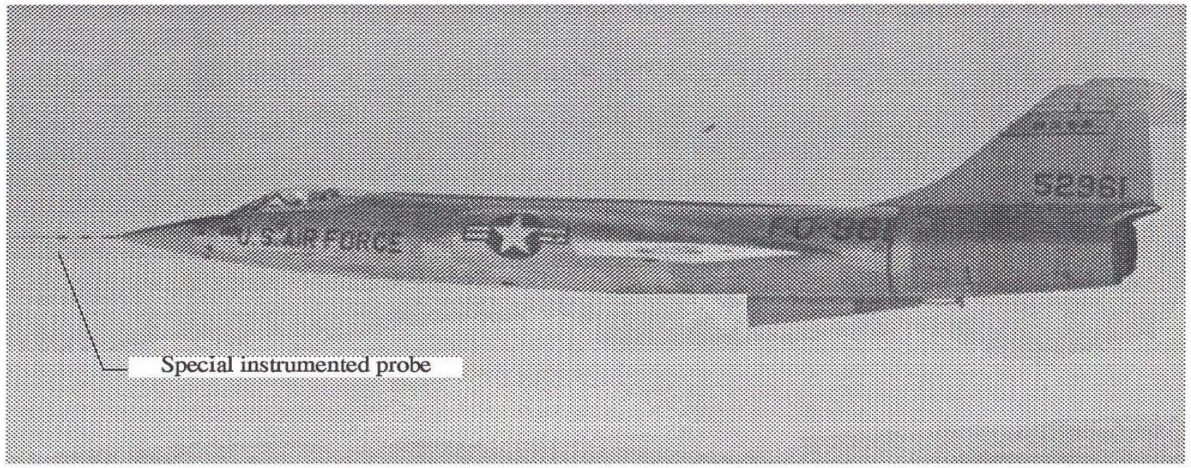

(a) Probe airplane

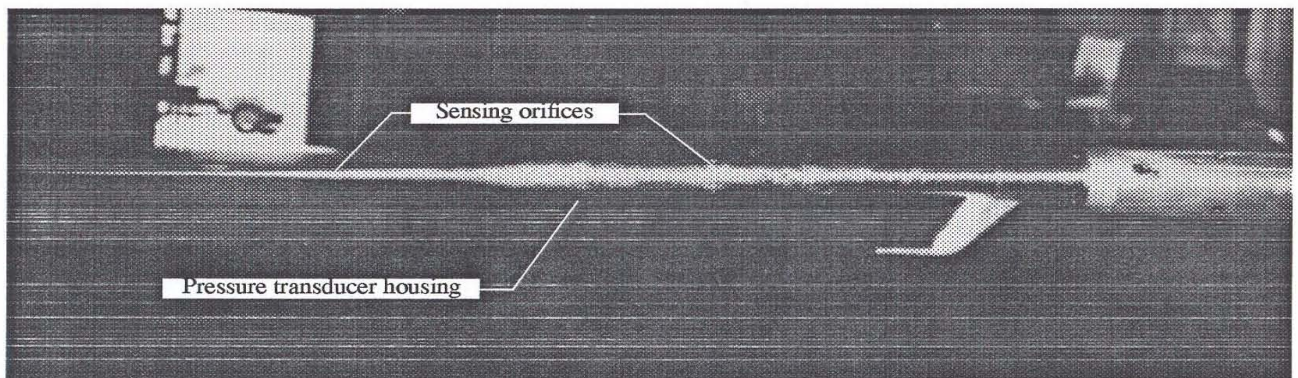

(Courtesy of NASA Flight Research Center)

(b) Probe used for in-flight pressure measurements

Figure 5.- F-104 fighter airplane with nose-boom probe installation for measuring the shock-flow-field in the vicinity of the disturbance-generating XB-70-1 airplane.

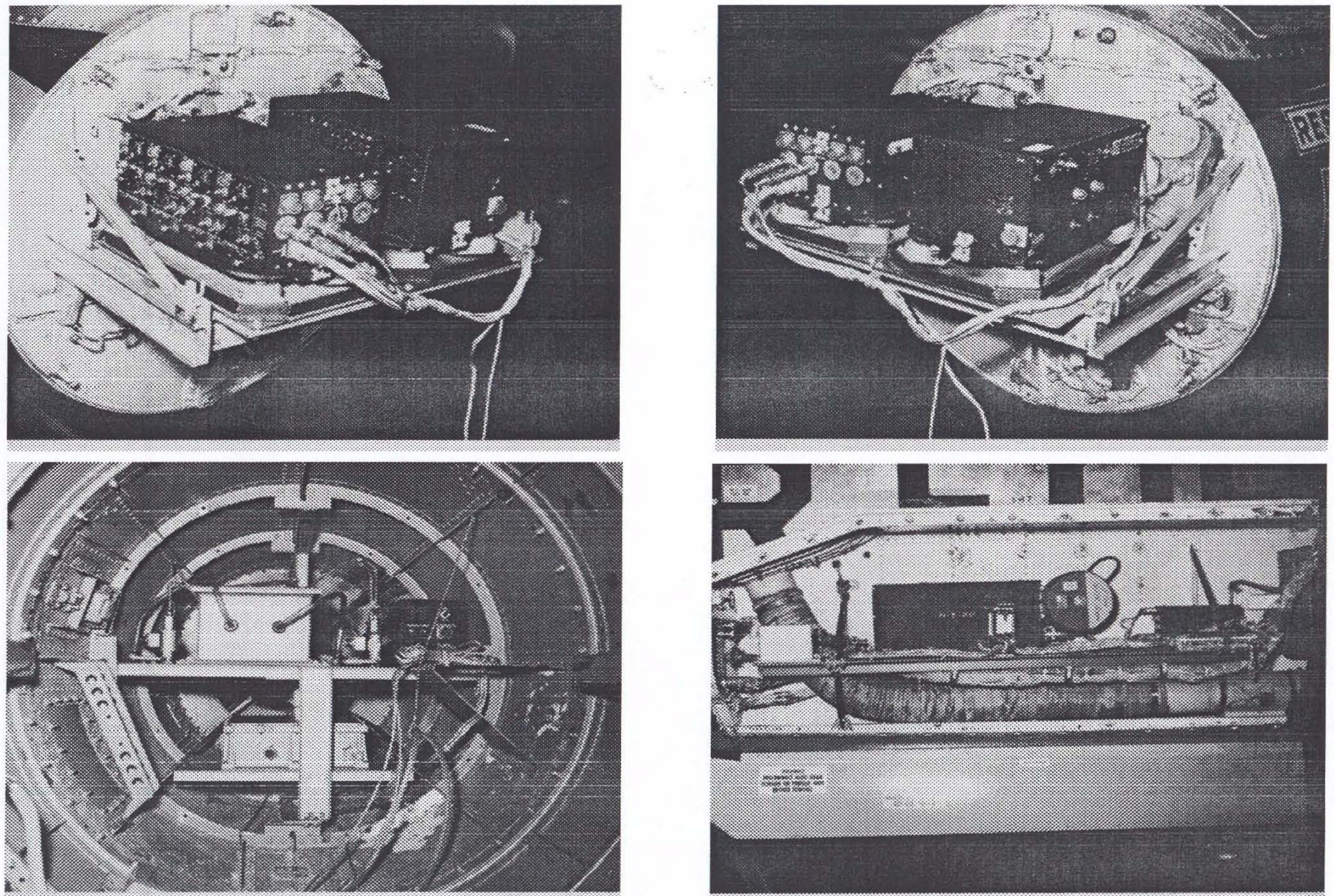

(Courtesy of NASA Flight Research Center)

Figure 6.- Photographs of the in-flight recording instrumentation mounted in the F-104 access bays.

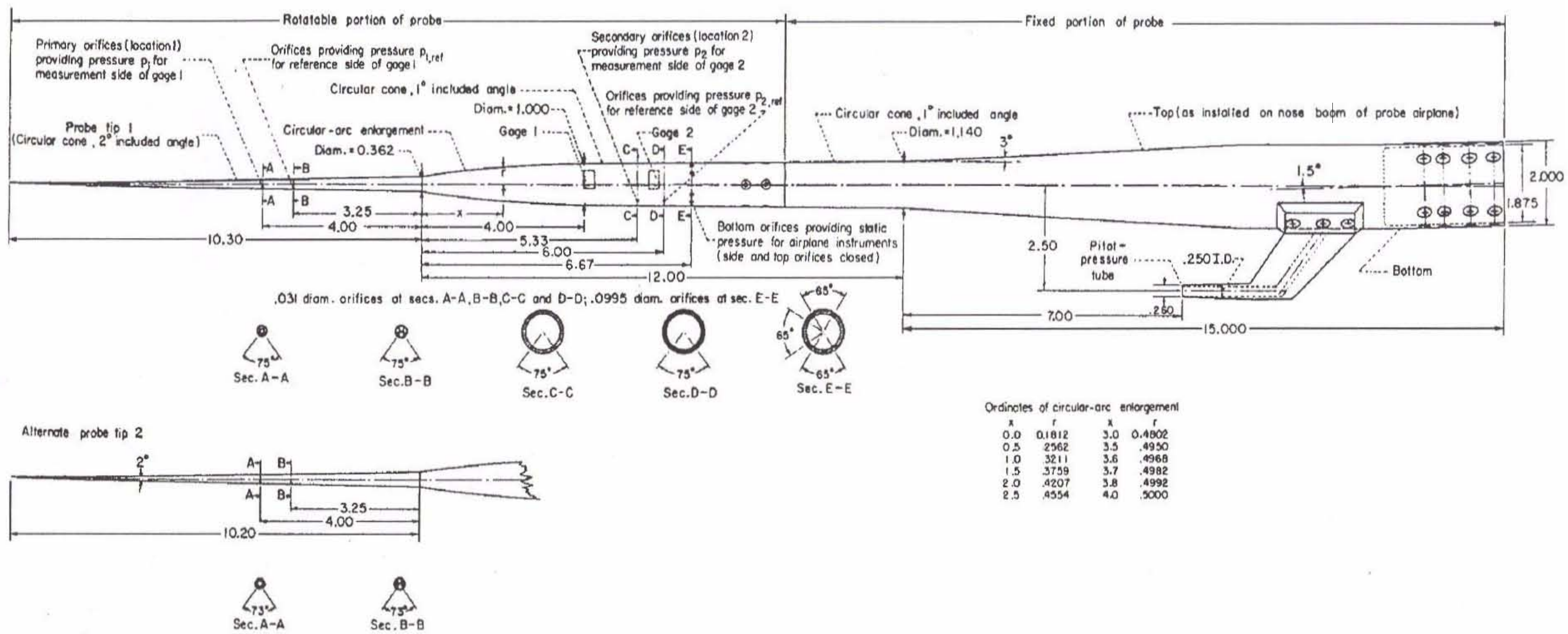

Figure 7.- Principal details and dimensions of full scale probe used for in-flight measurements and for wind tunnel tests at a Mach number of about 2.01 (rotatable portion of probe is positioned for probe-airplane flight over generating airplane). Dimensions are in inches.

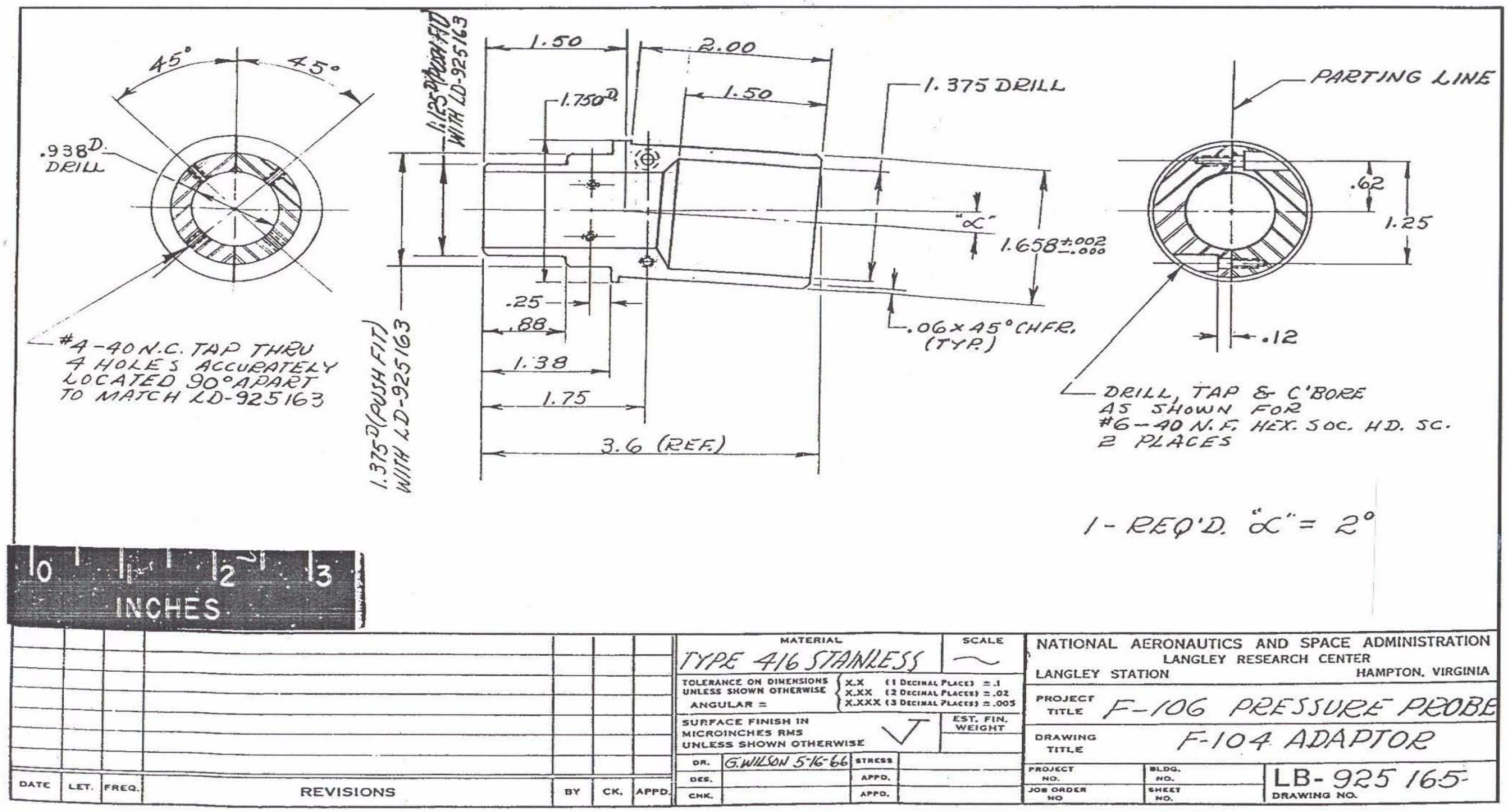

Figure 8.- Adaptor required to mate specially instrumented nose-boom pressure probe used originally on an F-106 to the NASA F-104 used in present tests.

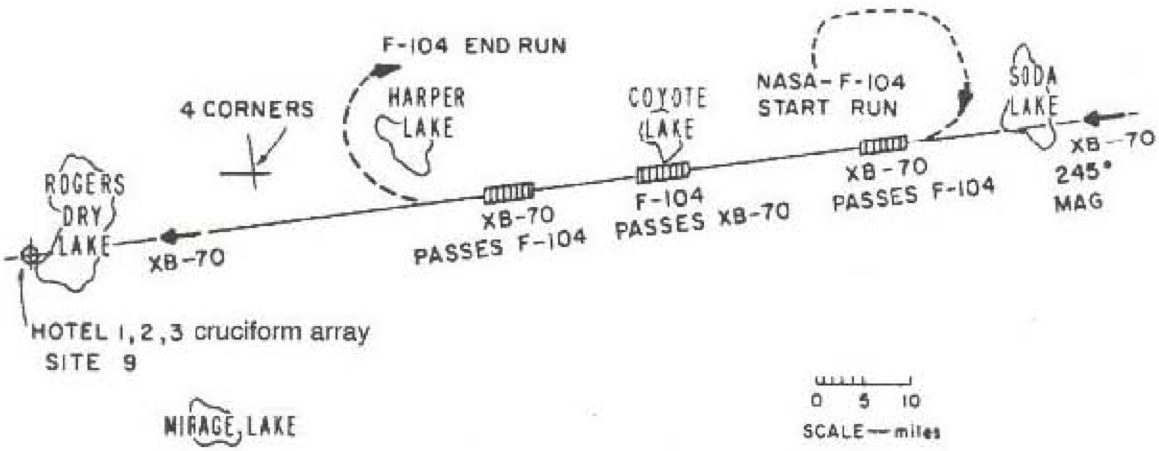

(a) General layout of probe missions relative to main test area.

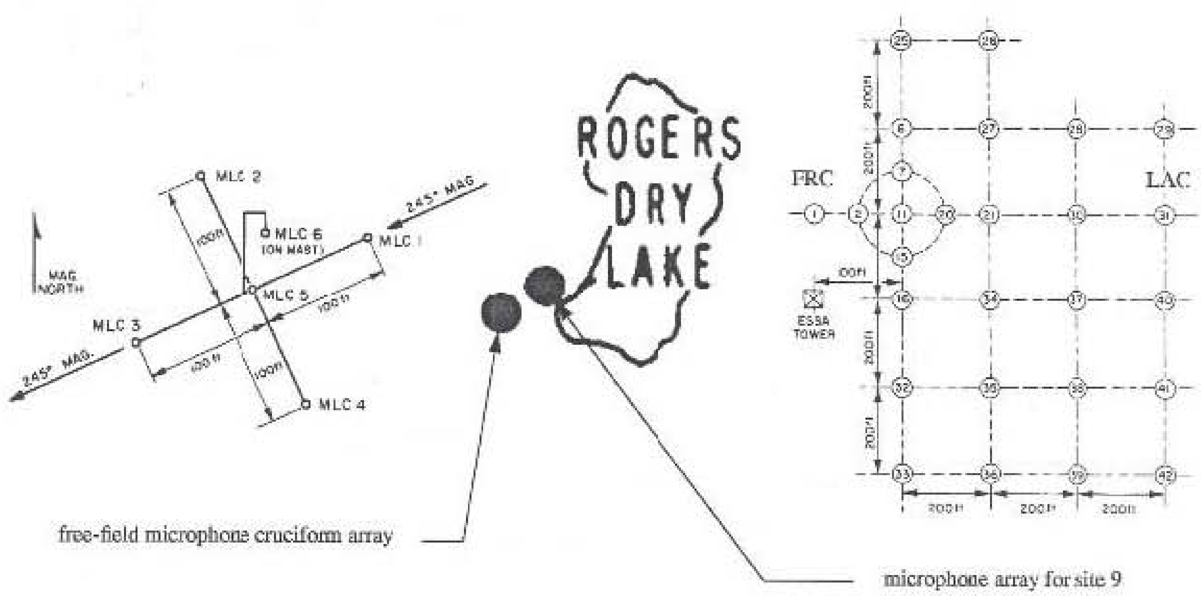

(b) Ground based microphone layouts at main test area.

Figure 9.- Schematic of XB-70 and F-104 nominal ground tracks showing area in which probe missions were flown and ground measurement were acquired.

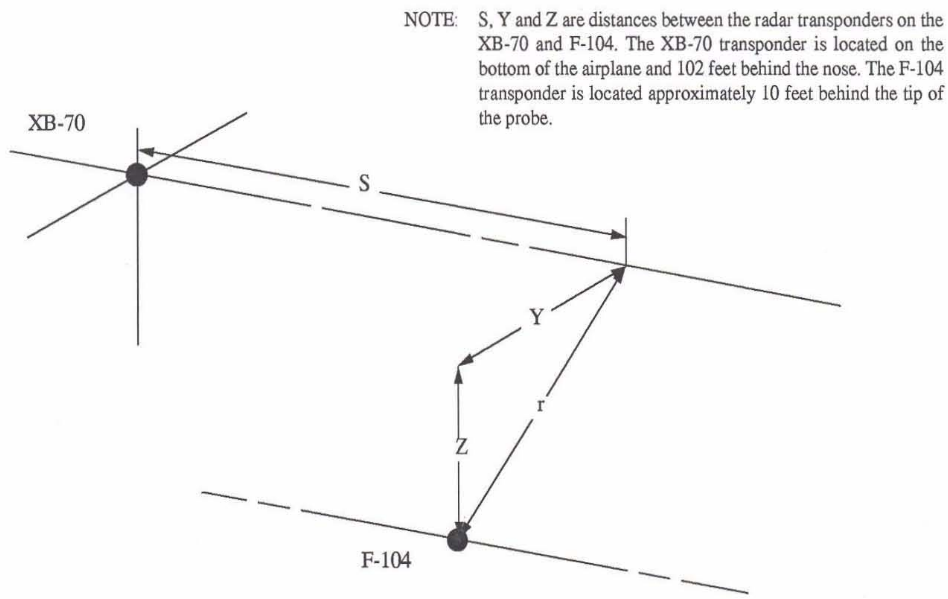

(a) XB-70 and F-104 coordinate system at time of penetration.

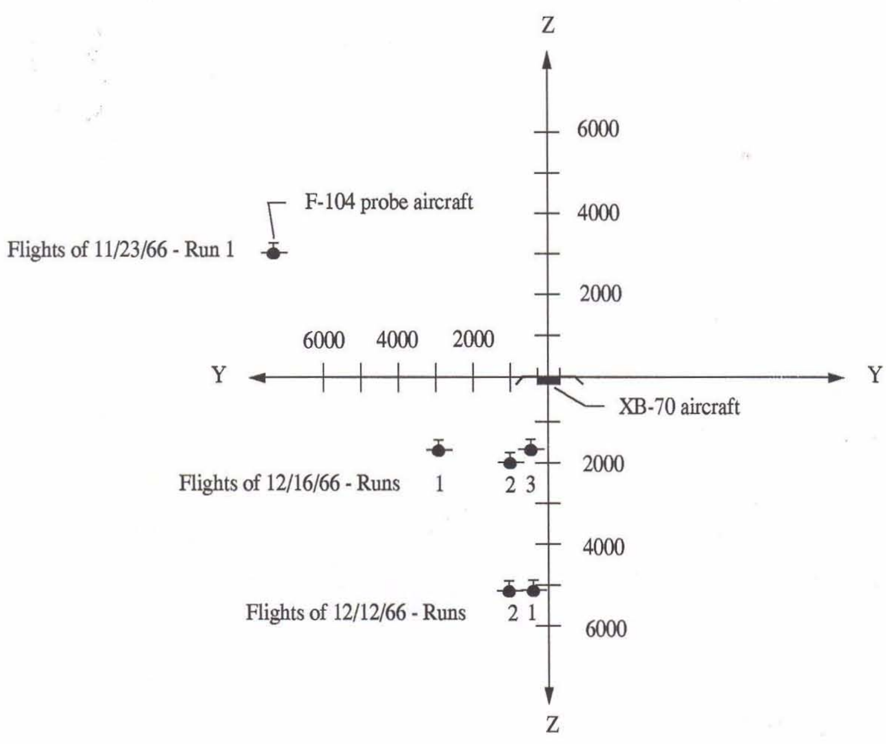

(b) Rear view in-flight direction showing F-104 probe runs relative to XB-70 flow field.

Figure 10.- Sketches illustrating general position of probe aircraft and generating aircraft.

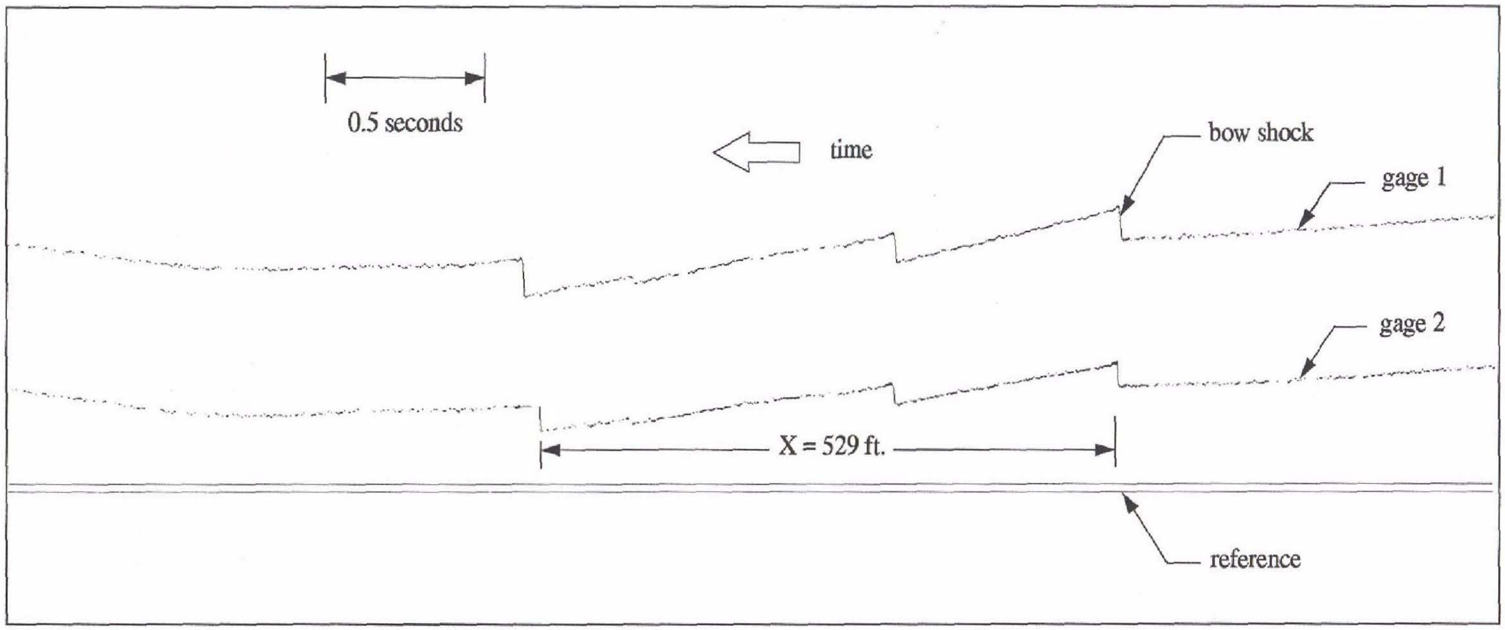

Pass 1, XB-70 overtakes F-104 probe aircraft (Z = -3290 ft., Y = 7100 ft., $r/l = 42$)

Figure 11.- Copy of November 23, 1966 film trace showing in-flight time histories of differential pressures measured in flow-field above XB-70 aircraft.

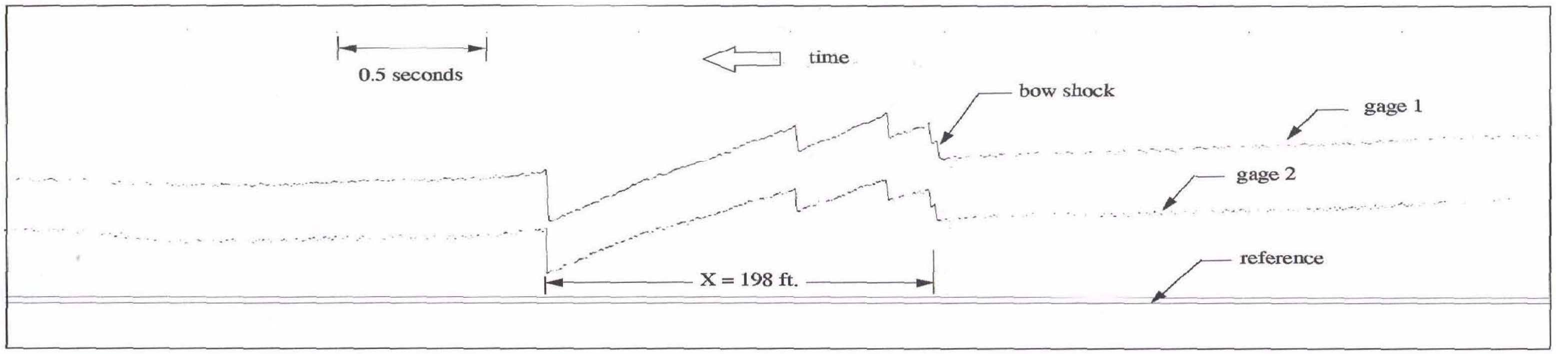

(a) Pass 1, XB-70 overtakes F-104 probe aircraft (Z = 4727 ft., Y = 220 ft., r/l = 26)

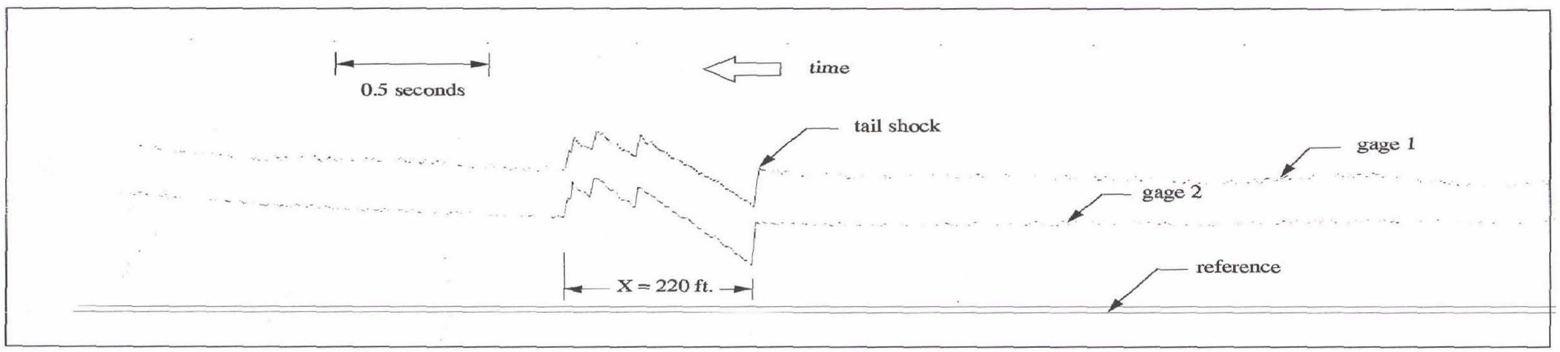

(b) Pass 2, F-104 probe aircraft overtakes XB-70 (Z = 4656 ft., Y = 825 ft., r/l = 26)

Figure 12.- Copy of December 12, 1966, film traces showing in-flight time histories of differential pressures measured in flow-field below XB-70 aircraft.

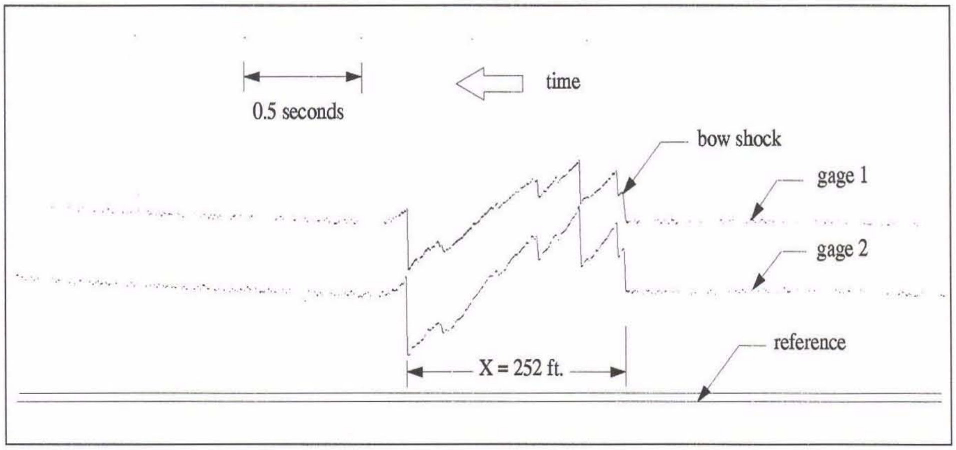

(a) Pass 1, XB-70 overtakes F-104 probe aircraft (Z = 1870 ft., Y = 2900 ft., r/l = 19)

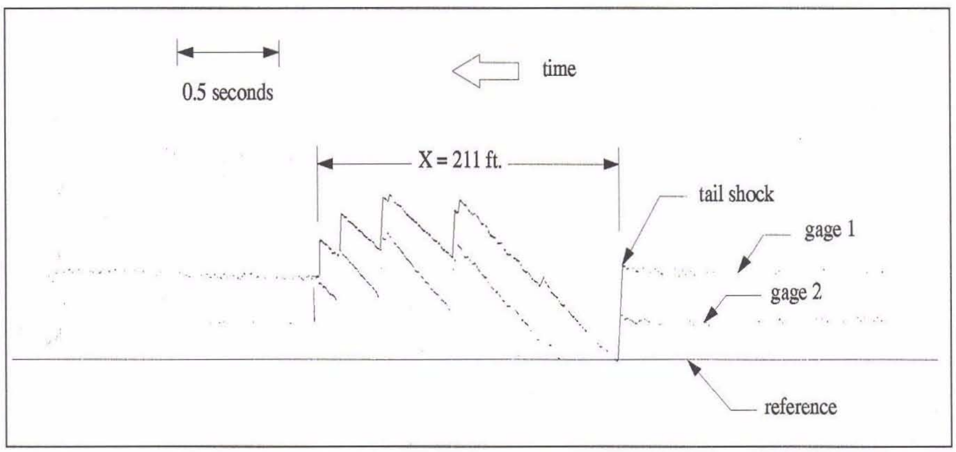

(b) Pass 2, F-104 probe aircraft overtakes XB-70 (Z = 2031 ft., Y = 980 ft., r/l = 12)

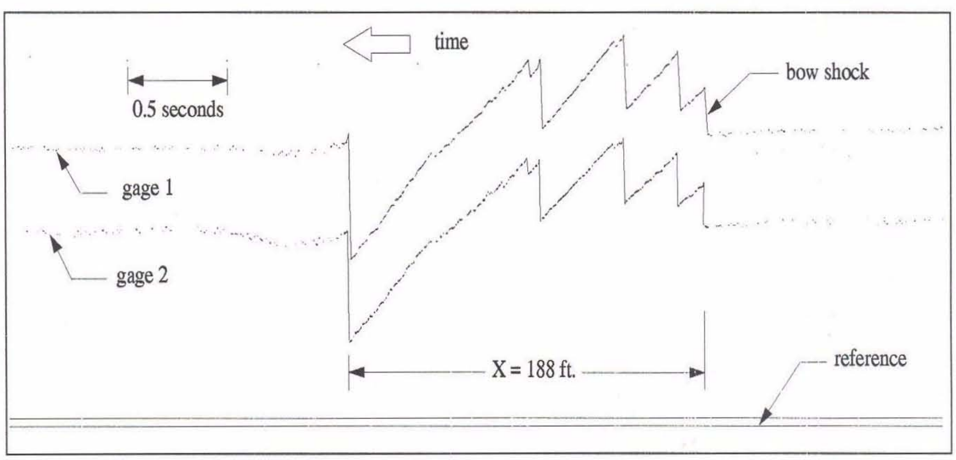

(c) Pass 3, XB-70 overtakes F-104 probe aircraft (Z = 1802 ft., Y = 590 ft., r/l = 10)

Figure 13.- Copy of December 16, 1966, film traces showing in-flight time histories of differential pressures measured in flow-field below XB-70 aircraft

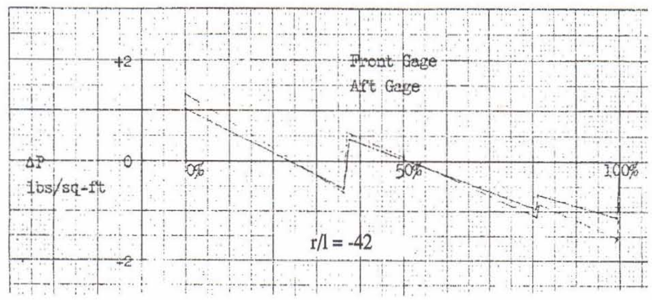

(a) Pass 1 on Nov. 23, 1966. Penetration time = 18:27:45 Z

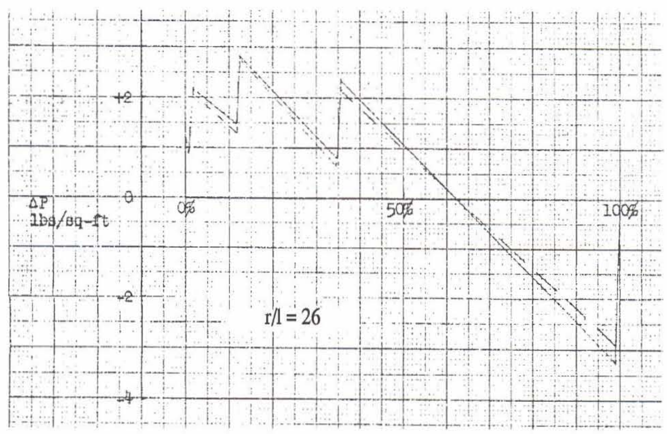

(b) Pass 1 on Dec. 12, 1966. Penetration time = 18:27:32 Z

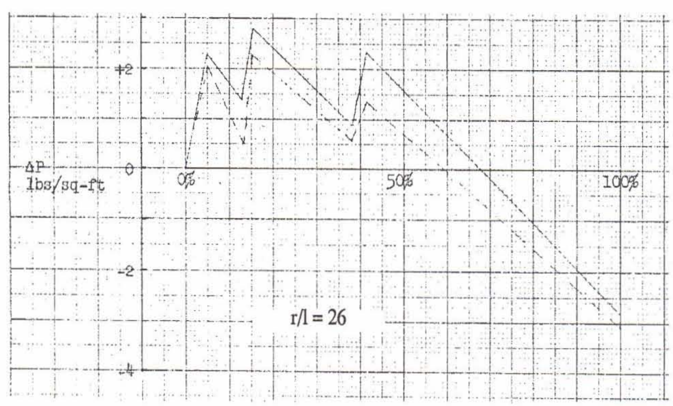

(c) Pass 2 on Dec.12, 1966. Penetration time = 18:29:18 Z

Figure 14.- XB-70 flow-field shock-wave signature overpressures.

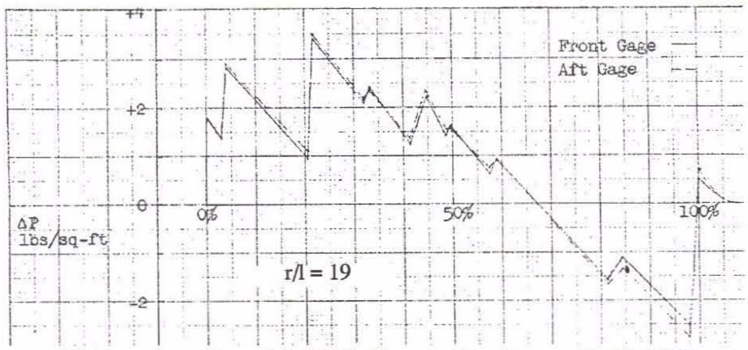

(d) Pass 1 on Dec. 16, 1966. Penetration time = 15:52:06 Z

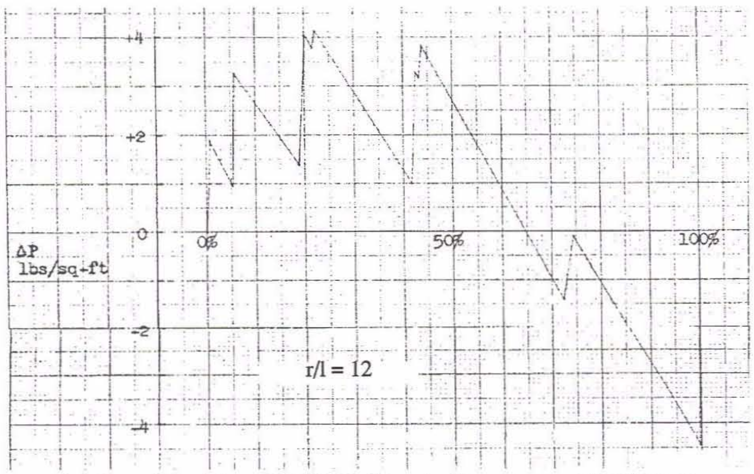

(e) Pass 2 on Dec. 16, 1966. Penetration time = 15:54:06 Z

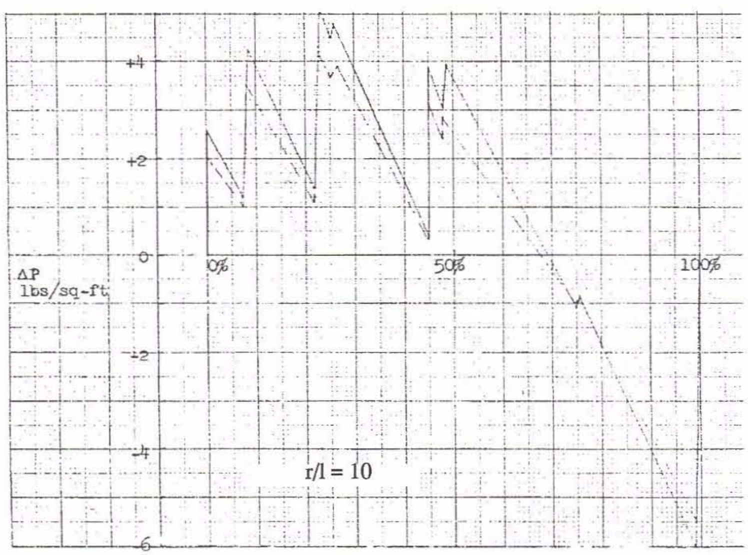

(f) Pass 3 on Dec. 16, 1966. Penetration time = 15:55:04 Z

Figure 14.- Concluded.

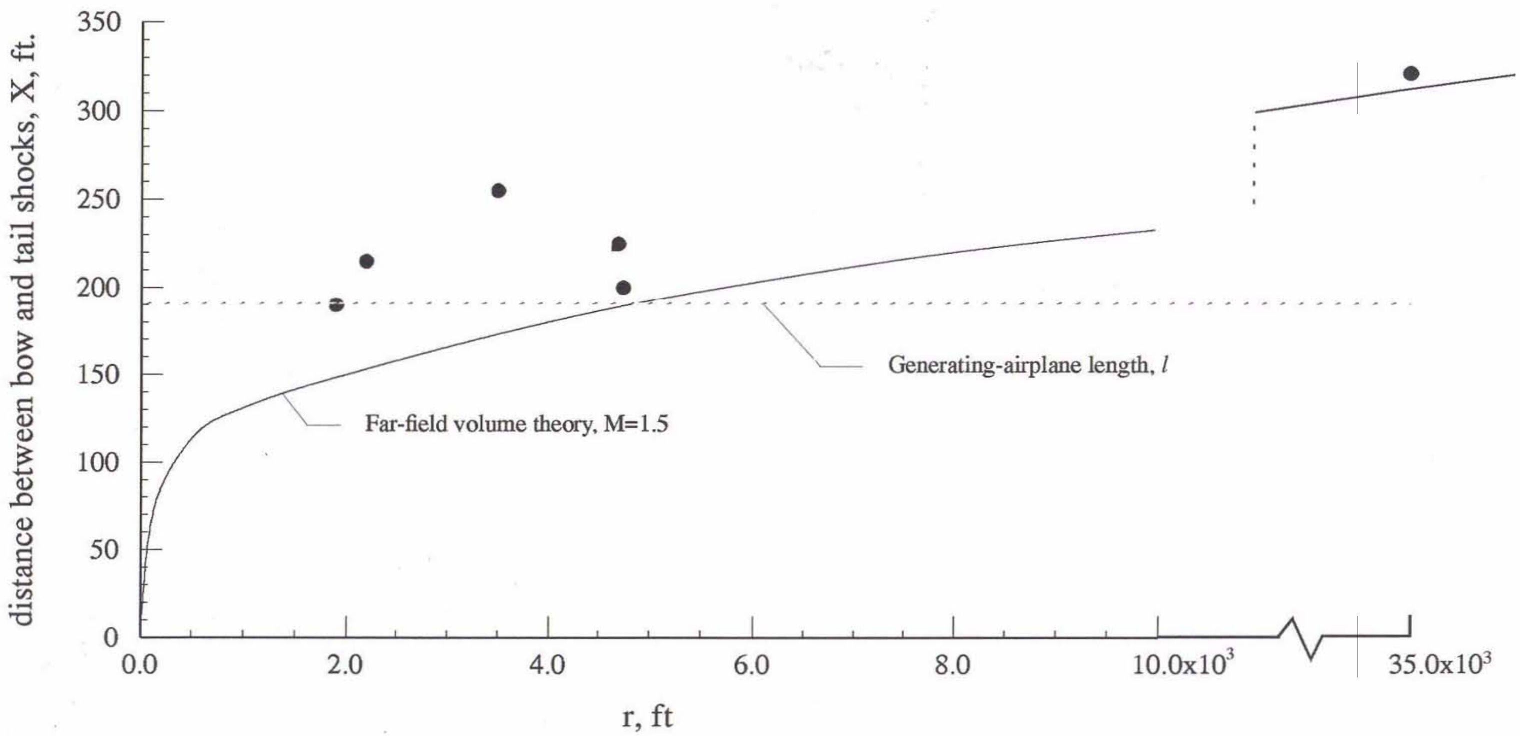

Figure 15.- Comparison of measured and calculated distances between bow wave and tail wave of generating airplane.

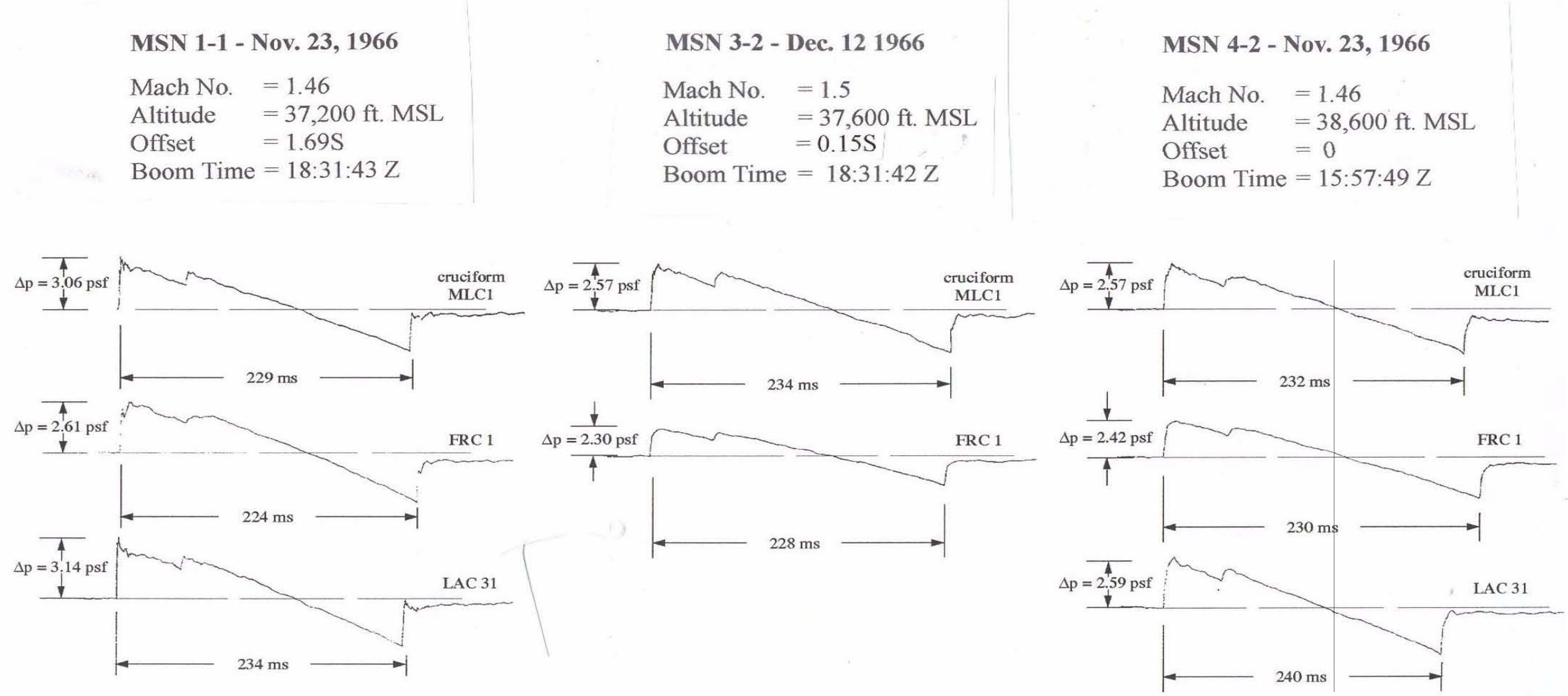

Figure 16.- XB-70 measured sonic boom signatures at ground level following in-flight probe tests.

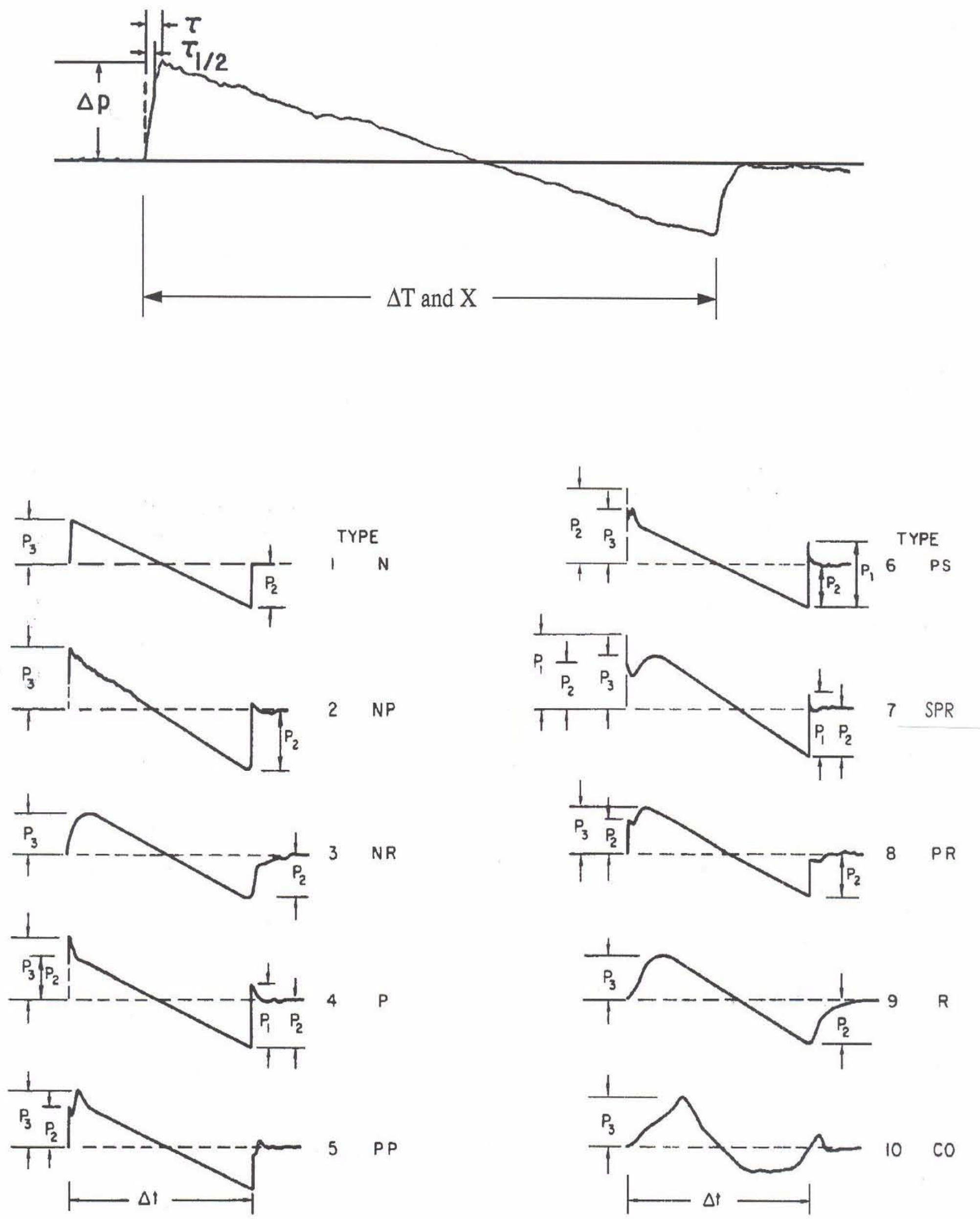

Figure 17.- Diagrams of waveforms and signature characteristics which represent the various categories of measured sonic booms.

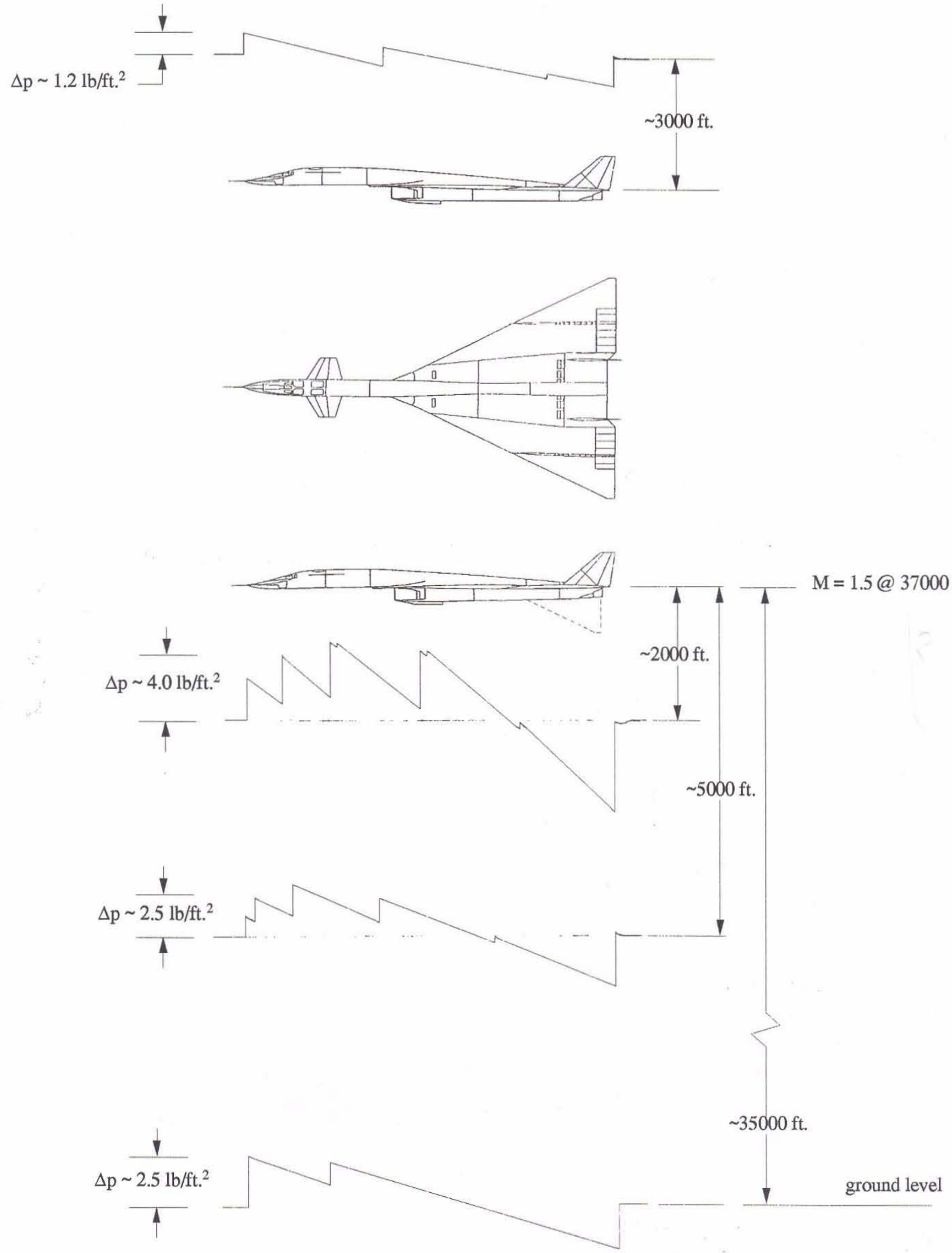

Figure 18.- Planform and side views of bomber airplane with time history of pressure signature as measured above and below the airplane. Signature length has been adjusted to make distance between nose and tail shocks approximately the same as the airplane length.

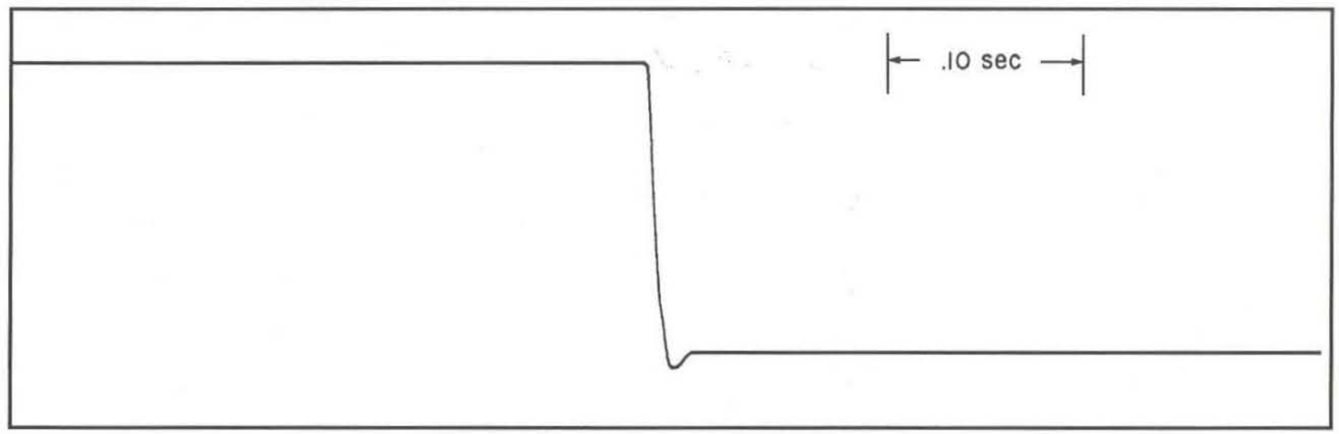

(a) Entire system (pressure gage and galvanometer).

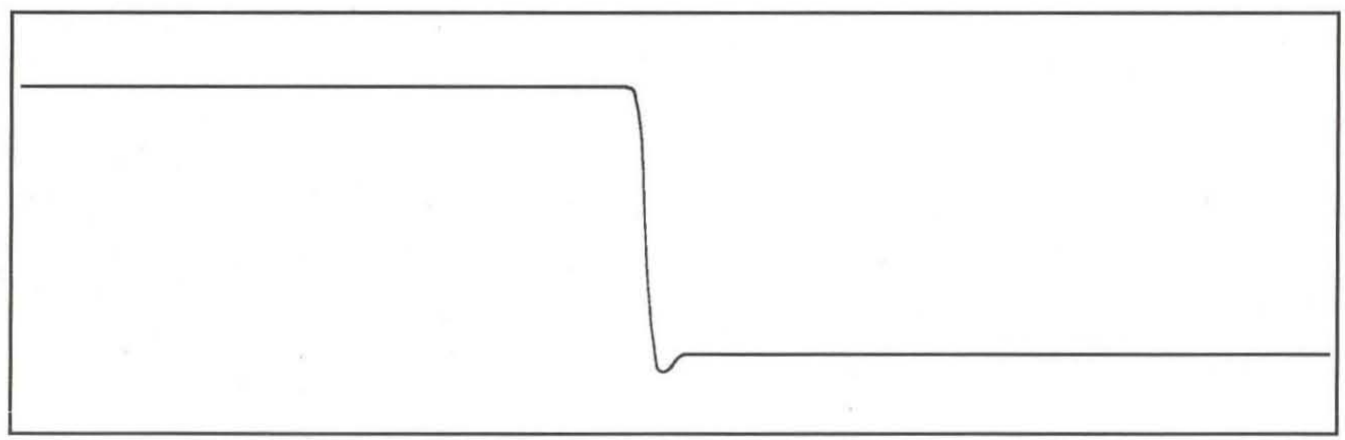

(b) Galvanometer only.

Figure 19.- Response characteristics of pressure instrumentation used for in-flight measurements.

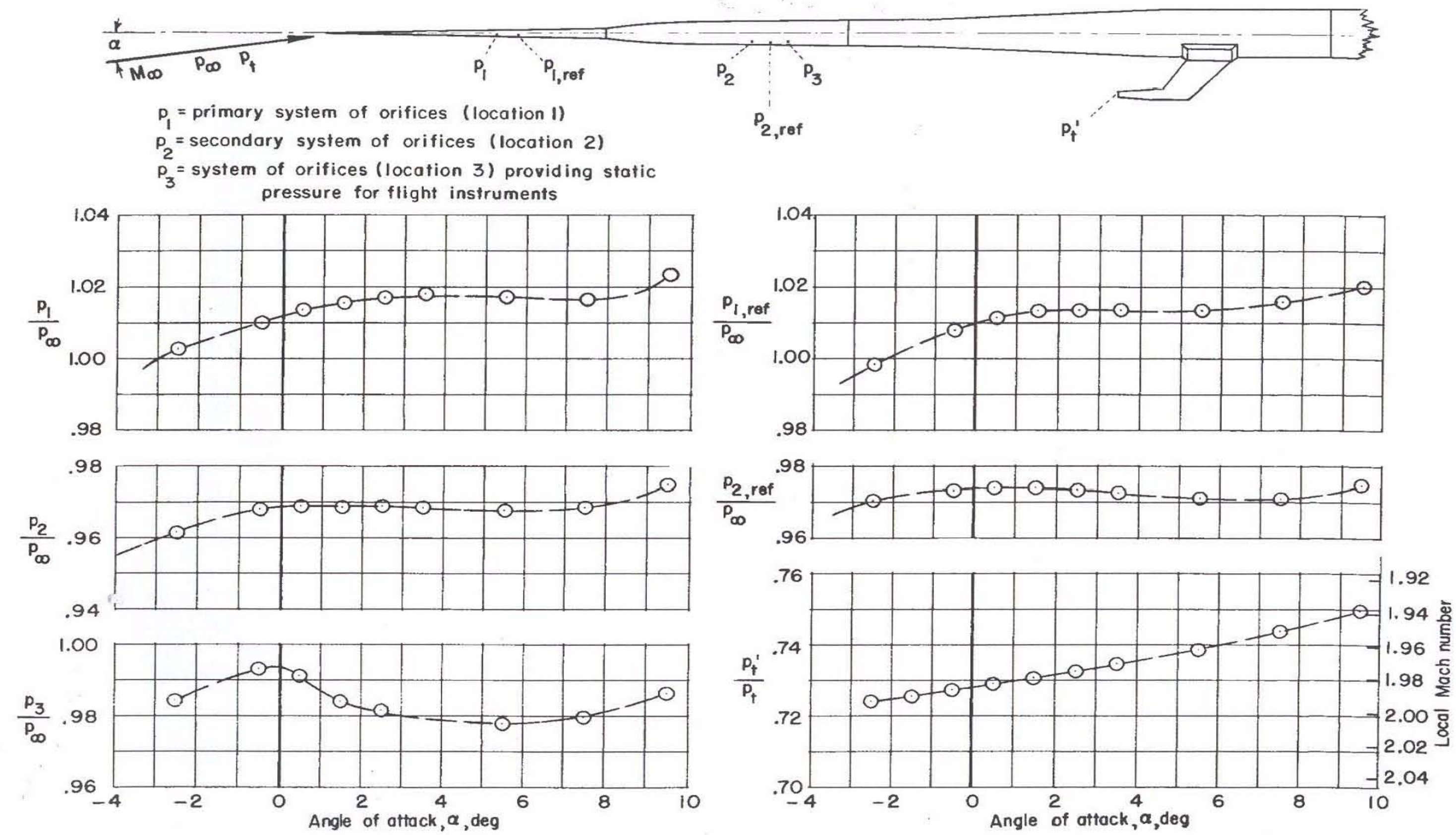

Figure 20.- Steady-state calibration of flight probe at angles of attack from -2.5° to 9.5°, as obtained from tests in the Langley 4-foot supersonic pressure tunnel (pressure orifices at bottom of probe). $M_\infty \approx 2.01$; $p_\infty \approx 185$ lb./sq. ft.

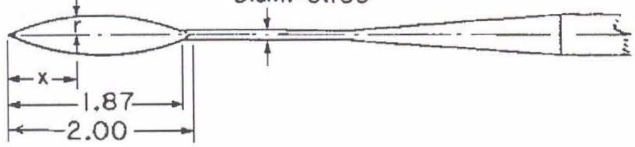

Body ordinates

x	r	x	r
0.00	0.000	1.00	0.200
.10	.038	1.25	.188
.25	.088	1.50	.150
.50	.150	1.75	.088
.75	.188	1.87	.050

(a) Disturbance-generating body of revolution (same shape as model D of ref. 27)

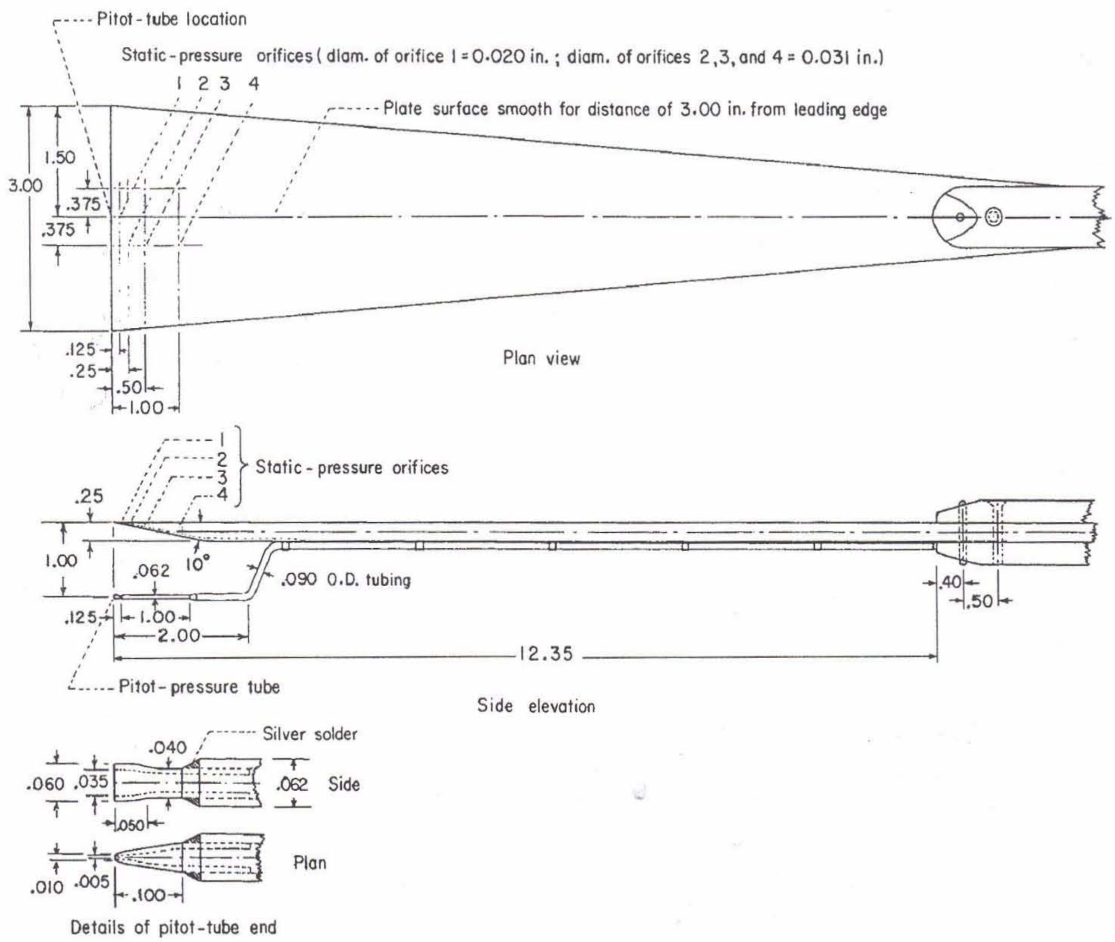

(b) Survey instrument for measuring pressure changes across body-generated disturbance.

Figure 21.- Wind-tunnel apparatus and test arrangement for generating and determining the strength of an axisymmetrical disturbance used in obtaining experimental evidence concerning the reflection characteristics of the flight probe. Dimensions are in inches.

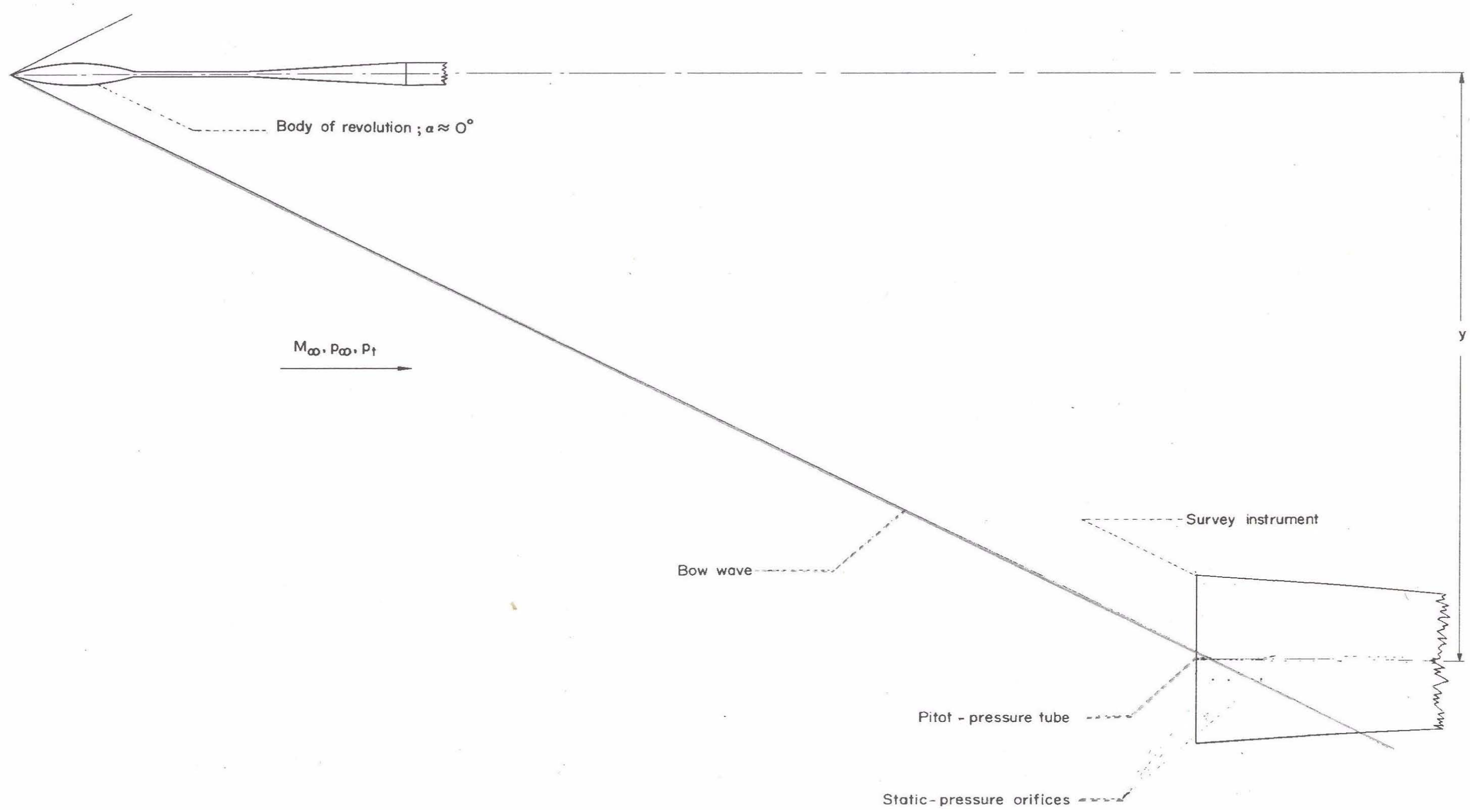

(c) Arrangement for measuring pressure changes across disturbance by use of survey instrument oriented to minimize wave-reflection effects.

Figure 21.- Concluded.

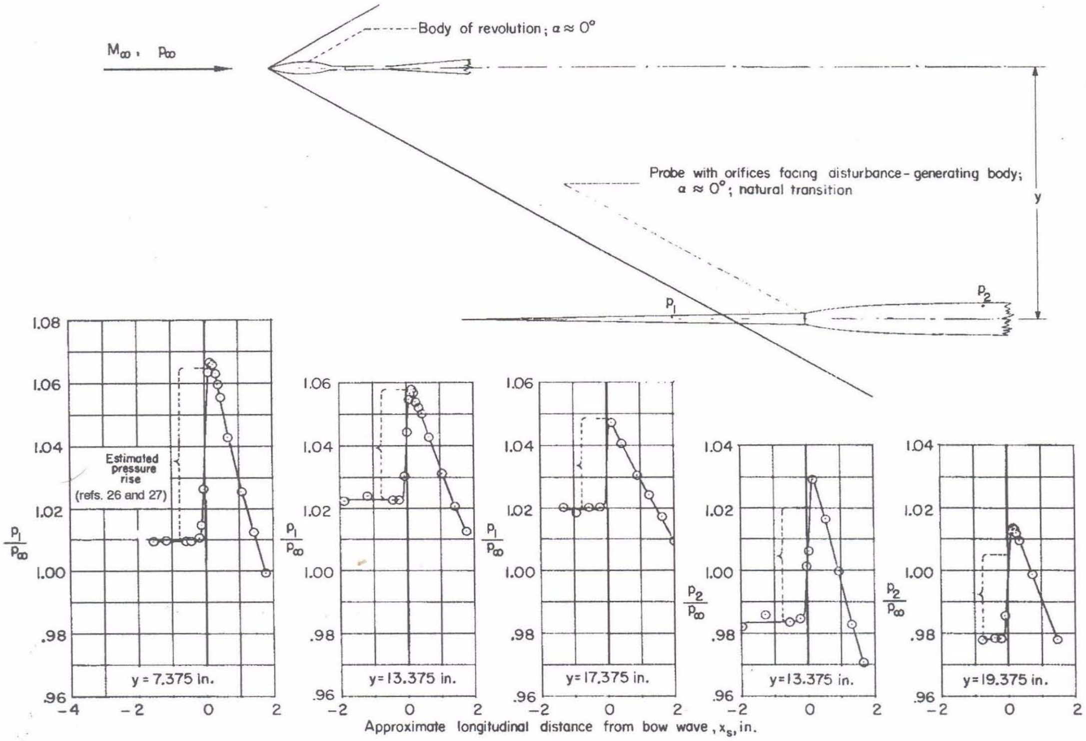

(a) Probe-indicated pressure changes across body-generated bow wave.

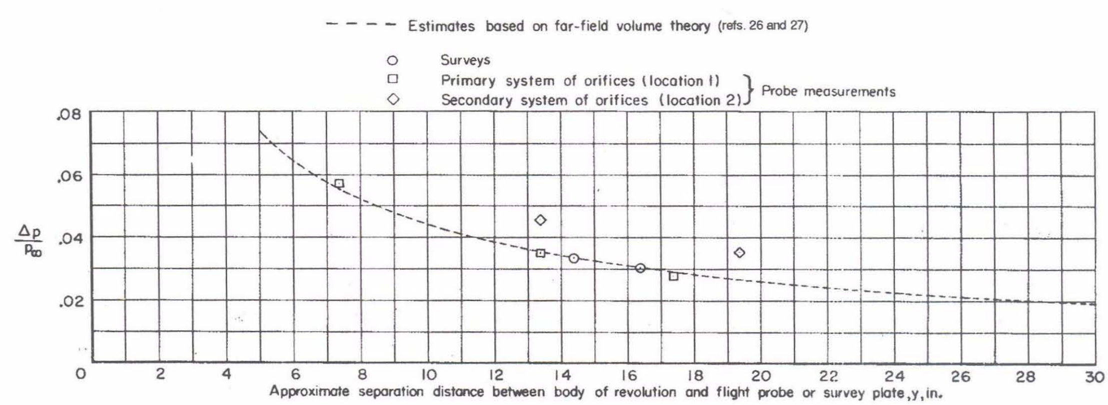

(b) Comparisons of estimated and measured maximum pressure rises across bow wave.

Figure 22.- Flight-probe capability for sensing static pressure changes across an axisymmetrical disturbance (bow wave generated by body of revolution), as evidenced by comparisons of probe-indicated, survey-indicated, and estimated pressure changes across bow wave. $M_\infty \approx 2.01$

REPORT DOCUMENTATION PAGE	*Form Approved* *OMB No. 0704-0188*

1. REPORT DATE *(DD-MM-YYYY)*	**2. REPORT TYPE**	**3. DATES COVERED** *(From - To)*
01- 04 - 2011	Contractor Report	

4. TITLE AND SUBTITLE
Measured Sonic Boom Signatures Above and Below the XB-70 Airplane Flying at Mach 1.5 and 37,000 Feet

5a. CONTRACT NUMBER
NNL07AE38T

5b. GRANT NUMBER

5c. PROGRAM ELEMENT NUMBER

6. AUTHOR(S)
Maglieri, Domenic J.; Henderson, Herbert R.; Tinetti, Ana F.

5d. PROJECT NUMBER

5e. TASK NUMBER

5f. WORK UNIT NUMBER
984754.02.07.07.11.01

7. PERFORMING ORGANIZATION NAME(S) AND ADDRESS(ES)
NASA Langley Research Center
Hampton, VA 23681-2199

Eagle Aeronautics, Inc.
13 West Mercury Boulevard
Hampton, VA 23669-2508

8. PERFORMING ORGANIZATION REPORT NUMBER

9. SPONSORING/MONITORING AGENCY NAME(S) AND ADDRESS(ES)
National Aeronautics and Space Administration
Washington, DC 20546-0001

10. SPONSOR/MONITOR'S ACRONYM(S)
NASA

11. SPONSOR/MONITOR'S REPORT NUMBER(S)
NASA/CR-2011-217077

12. DISTRIBUTION/AVAILABILITY STATEMENT
Unclassified - Unlimited
Subject Category 71
Availability: NASA CASI (443) 757-5802

13. SUPPLEMENTARY NOTES
Langley Technical Monitor: Peter G. Coen

14. ABSTRACT
During the 1966-67 Edwards Air Force Base (EAFB) National Sonic Boom Evaluation Program, a series of in-flight flow-field measurements were made above and below the USAF XB-70 using an instrumented NASA F-104 aircraft with a specially designed nose probe. These were accomplished in the three XB-70 flights at about Mach 1.5 at about 37,000 ft. and gross weights of about 350,000 lbs. Six supersonic passes with the F-104 probe aircraft were made through the XB-70 shock flow-field; one above and five below the XB-70. Separation distances ranged from about 3000 ft. above and 7000 ft. to the side of the XB-70 and about 2000 ft. and 5000 ft. below the XB-70. Complex near-field "sawtooth-type" signatures were observed in all cases. At ground level, the XB-70 shock waves had not coalesced into the two-shock classical sonic boom N-wave signature, but contained three shocks. Included in this report is a description of the generating and probe airplanes, the in-flight and ground pressure measuring instrumentation, the flight test procedure and aircraft positioning, surface and upper air weather observations, and the six in-flight pressure signatures from the three flights.

15. SUBJECT TERMS
Sonic boom; Sonic boom signatures; XB-70; Supersonic; Shock waves

16. SECURITY CLASSIFICATION OF:			**17. LIMITATION OF ABSTRACT**	**18. NUMBER OF PAGES**	**19a. NAME OF RESPONSIBLE PERSON**
a. REPORT	**b. ABSTRACT**	**c. THIS PAGE**			STI Help Desk (email: help@sti.nasa.gov)
					19b. TELEPHONE NUMBER ***(Include area code)***
U	U	U	UU	70	(443) 757-5802